DEPARTMENT OF INDUSTRIAL CHEMISTRY "TOSO MONTANARI"

SECOND CYCLE DEGREE IN

LOW CARBON TECHNOLOGIES AND SUSTAINABLE CHEMISTRY

CLASSE LM-71 - SCIENZE E TECNOLOGIE DELLA CHIMICA INDUSTRIALE

PRODUCTION OF JET BIOFUELS CATALYSED BY MOFS THROUGH THE GUERBET REACTION

Supervisor

Prof. Walter Zegada Lizarazu

Co-Supervisor

Prof. Iker Aguirrezabal

Candidate

Marco Montesi

Session January 2026

Academic Year 2024/2025

Contents

Acknowledgments

The experimental part of this thesis was carried out in the framework of the project of Pedro Cantarero Gómez, Pedro Luis Arias, Iker Aguirrezabal and Miryam Gil, aimed at developing a catalyst for ethanol upgrading to produce Sustainable Aviation Fuels (SAF). My contribution consisted in the characterization, impregnation and catalytic testing of the MOFs.

Abstract

The transition toward low-carbon transportation has stimulated growing interest in bio-based fuels capable of replacing fossil-derived hydrocarbons, particularly in sectors where electrification is not easily achievable. Among the possible technologies, the Guerbet reaction represents a promising strategy to convert short-chain alcohols such as ethanol into higher alcohols with improved fuel properties. In this work, the catalytic upgrading of ethanol to n-butanol was investigated using MOF-based catalysts under continuous gas-phase conditions.

A series of catalysts were synthesized by varying metal loading, impregnation procedures and catalyst dilution, and were tested in a fixed-bed reactor. The catalytic performance was evaluated in terms of ethanol conversion and product selectivity as a function of feed conversion, with particular attention to catalyst deactivation phenomena. Spectroscopic and compositional characterization techniques were employed to correlate catalytic behaviour with structural and chemical features of the catalysts.

The results show that MOF-based catalysts can promote the Guerbet coupling under relatively mild conditions compared to conventional heterogeneous systems, while displaying a complex evolution of activity and selectivity during operation. Analysis of selectivity and production rate trends indicates that catalyst deactivation plays a key role in shaping the product distribution, highlighting the sensitivity of the Guerbet pathway to the nature and stability of the active sites. These findings contribute to a deeper understanding of structure–performance relationships in MOF-derived catalysts and provide insights for the design of more stable and selective systems for biofuel upgrading.

1. Introduction

1. General Context: Energy and Transport Fuels in the European Union

Around 50 years ago, the scientific community recognized that human activities, driven by exponential population growth and industrial development, were beginning to exert a significant and measurable impact on natural equilibria. This realization, often traced to milestones like the 1972 United Nations Conference on the Human Environment, highlighted the need for sustainable practices to mitigate environmental degradation. In the EU, energy consumption and greenhouse gas (GHG) emissions remain central to this challenge, particularly in the transport sector, which among the largest contributor to GHG emissions and has shown limited progress in reductions over recent decades.

In 2023, the EU's transport sector accounted for approximately 25% of total GHG emissions, with road transport alone responsible for 73% of transport-related emissions [1]. Preliminary estimates for 2024 indicate a modest 0.7% increase in transport GHG emissions compared to 2023, highlighting the sector's ongoing reliance on fossil fuels [1]. Overall, EU GHG emissions in Q2 2025 were estimated at 772 million tonnes of CO2-equivalents, a slight 0.4% decrease from the previous year, but transport emissions remain high [2].

Looking at the future, EU energy consumption trends project significant shifts driven by the European Green Deal and “Fit for 55” package, aiming for a 55% GHG reduction by 2030 and climate neutrality by 2050. Primary energy demand in the EU is expected to decline by 30–47% from 2005 levels by 2050 across various scenarios, with electricity's share rising from 25% today to over 50% due to electrification [3] [4]. In transport, final energy consumption is projected to decrease by a 16% in 2030 compared to 2019 levels, driven by efficiency gains and fuel shifts [5]. However, without accelerated action, transport emissions could peak at nearly 800 million tonnes of CO2 in 2025 before falling by about 25% by 2035 [6].

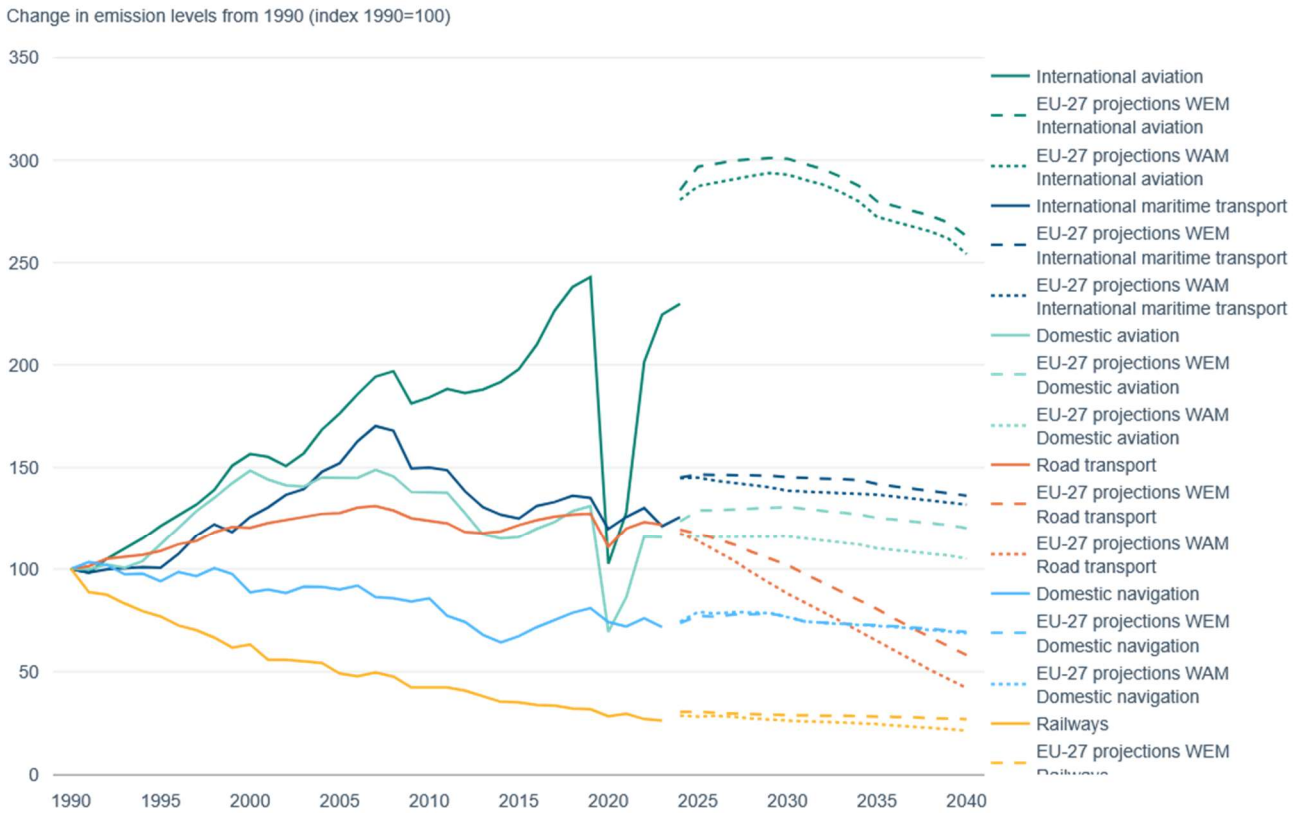

Figure 1 Greenhouse gas emissions from transport in the EU, by transport mode and scenario; Reused under the EEA Data Policy (Open Data Commons Attribution License)

2. The Need for Transition to Biofuels and Current Technological Possibilities

The transport sector's contribution to CO2 emissions—around 15–25% globally and in the EU [1] [7]—has prompted intensive research into sustainable solutions over the past two decades. Electrification is viable for light-duty vehicles and short-haul transport, but sectors like aviation and heavy-duty road transport face challenges due to insufficient battery energy density and infrastructure limitations [8]. Here, "carbon-neutral" fuels, or biofuels, emerge as a critical pathway, offering compatibility with existing engines and infrastructure while reducing lifecycle emissions.

Biofuels are defined as "a fuel, generally in liquid form, produced from biomass, including bioethanol from sugarcane, sugar beet or maize and biodiesel from canola or soybeans" [9], or more broadly as "combustible materials derived directly or indirectly from biomass (plants or organic wastes)" [10]. First-generation biofuels, produced via biological processes from sugars and organic waste, provide renewable alternatives but exhibit suboptimal properties: lower

energy density (e.g., ethanol at ~70% of gasoline's volumetric energy density), high water affinity, and limited miscibility with fossil fuels. These limitations necessitate further catalytic upgrading to advanced biofuels with enhanced stability, energy content and compatibility.

Current prominent technologies for sustainable aviation fuels (SAF)—a key focus due to aviation's hard-to-abate emissions—include:

- **Hydroprocessing of Esters and Fatty Acids (HEFA)**: Utilizes vegetable oils, animal fats, and waste oils. Advantages: Mature technology, high yields (up to 80–90% jet fuel fraction), and compatibility with existing refineries; it dominates current SAF production (over 90% of volumes). Disadvantages: Limited by feedstock availability (competes with food chains), high costs ($0.80–1.50/L vs. $0.50/L for jet fuel), and sustainability concerns if non-waste feedstocks are used [11] [12] [13] [14].
- **Fischer-Tropsch (FT)**: Converts syngas from biomass gasification into hydrocarbons. Advantages: Feedstock flexibility (e.g., municipal waste, agricultural residues), high-quality fuel output, and potential for near-zero emissions with carbon capture. Disadvantages: High capital investment ($500–1,000 million per plant), requires syngas purification, and low jet fuel selectivity without additional processing (max ~40% straight-run) [11] [12] [13] [15].
- **Alcohol-to-Jet (ATJ)**: Upgrades bioalcohols (e.g., ethanol, butanol) from sustainable feedstocks like lignocellulosic residues or organic waste. Advantages: Uses abundant, non-food-competing feedstocks; flexible and scalable; supports circular economy by valorising waste. Disadvantages: Economic viability tied to feedstock costs and availability; requires multiple steps (dehydration, oligomerization, hydrogenation), leading to higher energy inputs and costs ($1.00–2.00/L) [11] [12] [13] [16].

  These technologies offer emission reductions of 50–80% on a lifecycle basis compared to fossil jet fuel, but challenges include high production costs (2–4 times fossil equivalents), feedstock constraints, and the need for policy incentives like blending mandates [14] [17]. Expanding biofuel adoption

requires innovations to improve selectivity, reduce purification needs, and lower environmental impacts.

3. Motivation of the Work: Selecting the Guerbet Route as an Alternative

Among biofuel pathways, the ATJ route stands out for its potential to leverage abundant bioethanol from sustainable sources without competing with food production. Within ATJ, the Guerbet reaction—upgrading ethanol to n-butanol—offers a compelling alternative to traditional processes. The Guerbet pathway involves tandem dehydrogenation, aldol condensation, dehydration and hydrogenation (shown in Figure 2), converting short-chain alcohols into higher alcohols with doubled carbon chains [18].

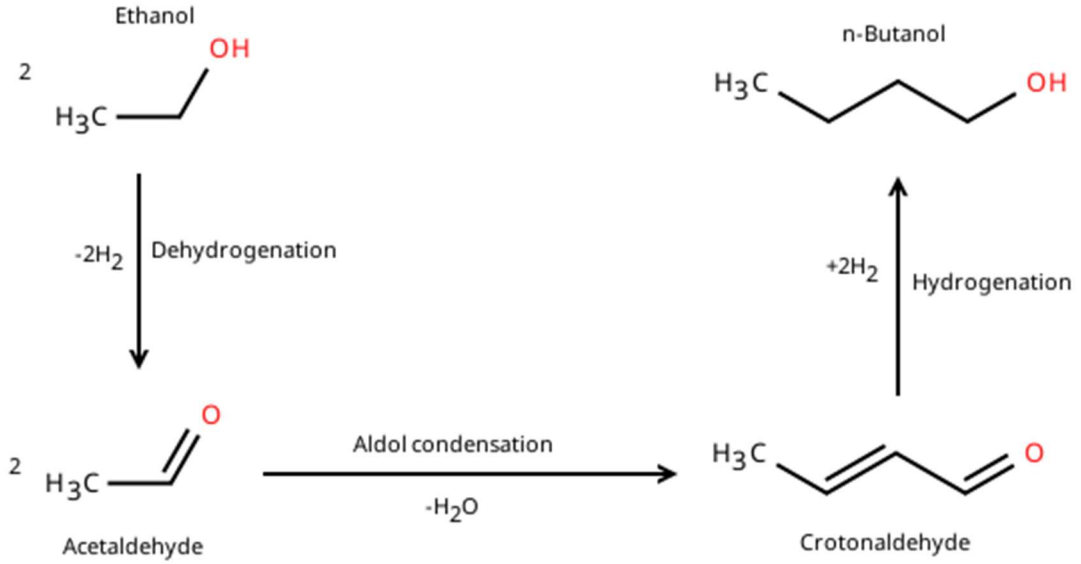

Figure 2 Guerbet reaction scheme adapted from Dahao et Al. [19]

This route addresses key limitations of bioethanol: n-butanol has a higher volumetric energy density (26.8 MJ/L vs. 21.1 MJ/L for ethanol), lower vapor pressure, reduced corrosiveness, and better miscibility with fossil fuels, making it an ideal precursor for jet fuels [18] [20]. Advantages include:

- **Efficiency and Selectivity**: High yields (up to 35–48% butanol selectivity) under mild conditions (e.g., 80–250°C), with catalysts like Mg-Al spinels or ruthenium complexes achieving 90%+ selectivity and long-term stability [18] [21].

- **Sustainability**: Utilizes bioethanol from waste biomass, minimizing land-use competition; low CO2 footprint compared to FT or HEFA, as by-products are minimal [20] [22].
- **Economic Potential**: Avoids high-capital costs, syngas purification (vs. FT) and feedstock scarcity (vs. HEFA); compatible with continuous processes for scalability [18] [23].

For aviation, Guerbet-derived butanol serves as a jet fuel precursor, enabling "alcohol-to-jet" SAF with lifecycle emissions reductions of 70–80% [16]. This motivates our focus on the Guerbet route in a continuous flow fixed-bed reactor, targeting ethanol-to-butanol conversion to reduce plane transport's environmental impact—a sector hard to electrify due to battery limitations [8].

4. Metal-Organic Frameworks (MOFs) as a Promising Catalytic Platform

Research on MOFs has surged in the last decade, with publications growing exponentially, positioning them as tunable platforms for complex reactions like the Guerbet process. MOFs, such as UiO-66, which combine metallic centres (e.g., Zr) with organic ligands, allowing modulation of crystallinity, acidity, and porosity to enhance activity and selectivity. For instance, lower crystallinity improves proton mobility [24], while tuned acidity favours aldol condensation and rapid adsorption/desorption.

In this work, we employ UiO-66 with palladium and copper co-catalysts for ethanol-to-butanol upgrading. This addresses biofuel challenges by improving energy density, stability, and water affinity. However, MOFs, due to their organometallic nature, face some limitations:

- Thermal stability: Organic ligands limit high-temperature resilience.
- Chemical stability: Susceptibility to water, acids, or bases.
- Synthesis and scalability: Complex, solvent-intensive processes.
- Reusability: Rapid structural degradation.

Despite these, MOFs' synergy (e.g., Pd for dehydrogenation/hydrogenation, Zr sites for condensation) offers superior performance under mild conditions, as

demonstrated in studies like Pd@UiO-66 achieving 50% butanol selectivity [19]. The following sections detail our experimental approach in a continuous flow reactor, aiming to advance SAF production and aviation sustainability.

2. Literature Review

1. Overview of Published Work on Ethanol Upgrading via Guerbet Reaction

The Guerbet reaction, a chain-growth process for upgrading light biomolecules like ethanol to higher alcohols such as n-butanol, has been extensively studied in catalysis and biofuels literature since its discovery over a century ago. This reaction is not novel, with abundant research covering a wide variety of catalysts, conditions, and feeds. As highlighted in recent mechanistic studies, such as those on defective Zr-MOFs [25], the Guerbet pathway typically involves acetaldehyde intermediates formed via ethanol dehydrogenation, followed by aldol condensation to crotonaldehyde, and subsequent hydrogenation. These steps require synergistic active sites: for instance, surface μ_1-OH groups act as key species for aldol condensation, working in concert with Zr^{4+} Lewis acid centres to achieve high selectivity (>90% to crotonaldehyde) under low-conversion conditions. Capillary condensation within the MOF's pores further enhances performance by facilitating product desorption, preventing side reactions and improving overall efficiency [25]. Such insights highlight the potential of tunable heterogeneous catalysts like MOFs, but also reveal ongoing challenges in scaling and optimizing for industrial biofuel production.

Published work on ethanol upgrading can be broadly categorized into homogeneous, tandem (homogeneous-heterogeneous), and fully heterogeneous approaches. Homogeneous catalysts, often transition metal complexes (e.g., ruthenium or iridium-based systems), excel in batch processes, achieving high yields due to precise control over reaction intermediates. For example, bifunctional iridium catalysts with nickel or copper hydroxides have reported ethanol conversions of ~37% and n-butanol selectivities exceeding 99% at mild temperatures (150–180°C) [26]. These systems promote efficient dehydrogenation/hydrogenation via metal hydrides and base-catalysed aldol steps, minimizing byproducts like sodium acetate or C_6+ alcohols [23]. However, their batch nature requires large reactors and reactant volumes for scalability, limiting industrial viability [26] [27].

Heterogeneous catalysts, including mixed metal oxides (e.g., Mg-Al spinels), hydroxyapatite (HAP), and emerging MOFs with metal nanoparticles, offer advantages in continuous processes, facilitating easier scale-up without additional reactants beyond the alcohol feed. Mixed oxides derived from hydrotalcite precursors have shown promise: for instance, Cu-doped Mg-Al catalysts achieve 26–41% ethanol conversion and 65–70% n-butanol selectivity at 200–280°C, with the metal favouring hydrogenation and the oxide providing acid-base sites for condensation [28] [18] [29]. HAP catalysts, with tunable Ca/P ratios, operate in gas-phase continuous modes at 350–450°C, yielding 1–15% conversion and ~50% selectivity, where surface phosphates stabilize enolates for aldol steps [30] [31]. MOF-based systems, such as Pd@UiO-66, enable milder conditions (e.g., 170–250°C, 2 MPa in continuous), with conversions up to 50% and selectivities of 48–99% over extended runs (e.g., 200 h), attributed to confined Pd nanoparticles for dehydrogenation/hydrogenation and Zr Lewis acid sites for condensation [32] [19] [25].

To compare these approaches with the present work, Table 1 summarizes key publications on alcohol upgrading. It highlights variations in catalyst type, temperature, pressure, phase/process, feed conversion, and n-butanol selectivity. For completeness, additional entries from recent literature have been included (e.g., Mg-Al spinels and RuNi@MOF), showing the range of performances.

Catalyst	Catalyst type	Temperature (°C)	Pressure (kPa)	Phase-Process	Conversion of feed	Selectivity towards n-butanol
Hydroxyapatite [30]	Heterogeneous	350-450	101	Gas-continuous	1-15%	50%
Transition metal complexes [26]	Homogeneous	150-180	Not specified	Liquid-batch	37%	99%
MOF + metal nanoparticles [32]	Heterogeneous	170	Not specified	Liquid-batch	27%	99%
Mg-Al spinel Pd doped [18]	Heterogeneous	200-280	3000	Liquid-continuous	17-26%	65-80%
RuNi@MOF [32]	Heterogeneous	<200	Not specified	Liquid-batch	Up to 31%	>90%
MOF + metal nanoparticles (this work)	Heterogeneous	250	2160	Gas-continuous	33-39% (over a 60h test)	27% (average over 60 h)

Table 1 comparison of publications related to alcohol upgrading for comparison with the present work

This table illustrates the trade-offs: homogeneous systems offer superior selectivity but poor scalability, while heterogeneous ones enable continuous operation at the cost of lower yields. For instance, HAP and mixed oxides require harsh temperatures (up to 580°C) and pressures (6–14 MPa) to achieve even modest conversions [28] [30] [31], whereas MOFs like UiO-66 with Pd nanoparticles operate under milder conditions (e.g., 250°C, 2 MPa), yielding 33-39% conversion and 27% average selectivity over 60 h.

Despite these results, published studies consistently highlight critical issues that hinder practical application:

- **Lack of Catalyst Stability**: Many heterogeneous catalysts suffer from deactivation over time. For example, metal sintering in Pd-doped mixed oxides leads to activity loss after 20–50 h [18], while HAP experiences phosphate leaching under high temperatures, reducing longevity [30] [31]. In MOFs, thermal/chemical instability (e.g., ligand degradation at >300°C or in aqueous environments) limits reuse. Homogeneous systems degrade via air/moisture sensitivity, requiring inert conditions impractical for industry [26] [27].
- **Poor Product Selectivity**: Side reactions dominate, producing unwanted byproducts like ethylene (from dehydration), diethyl ether, or C_6+ alcohols (from over-condensation). Homogeneous catalysts minimize this via precise

site control but still form acetates [23]; heterogeneous ones, especially oxides, yield <70% selectivity due to unbalanced acid-base sites favouring dehydration over aldol steps [28] [18] [29].

- **Poor Understanding of the Catalytic System**: The reaction mechanism is cause of debate, with no consensus on pathways (e.g., acetaldehyde self-condensation vs. ethanol-acetaldehyde coupling, which are shown in figure 3 along with a semi-direct coupling mechanism) or active sites. While synergies like Pd for hydrogen activation and Zr^{4+}/μ_1-OH for aldol are proposed [19] [25], variations across catalysts (e.g., MPV reduction in HAP [33] [31]) complicate optimization. This lack of mechanistic clarity hinders rational design, making predictive catalyst development hard to achieve [28] [27] [34]. These challenges—stability, selectivity, and mechanistic ambiguity—highlight the need for innovative catalysts that balance performance with scalability, particularly in continuous processes for biofuel production.

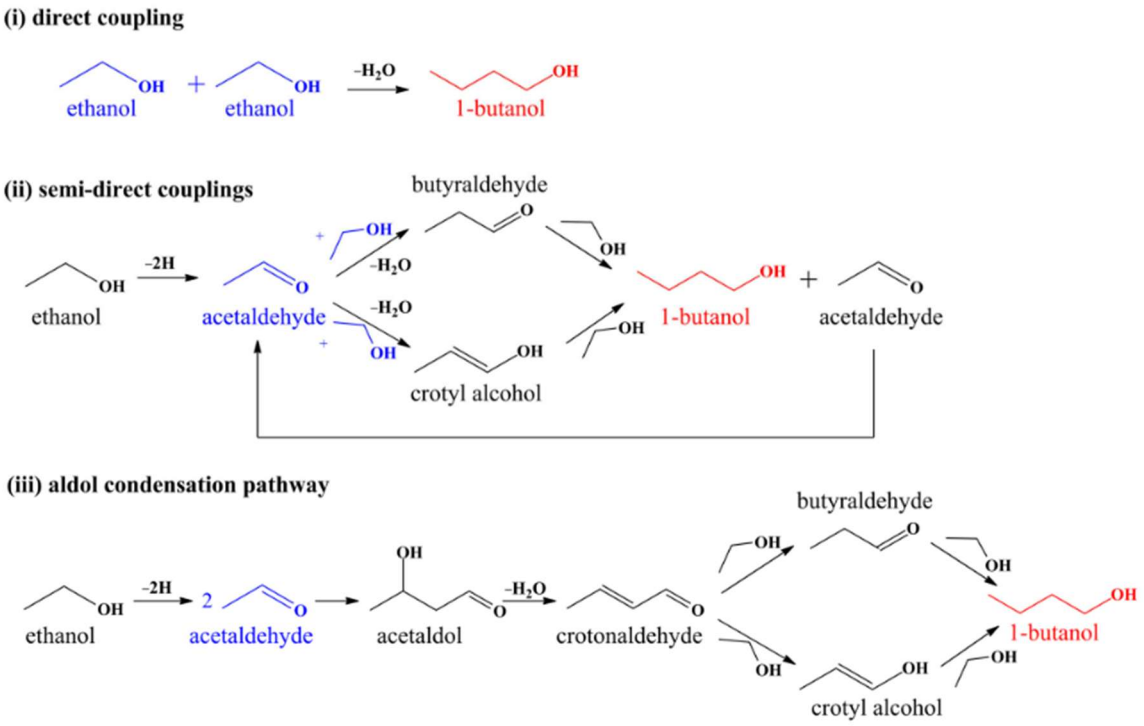

Figure 3. Mechanistic scheme of ethanol Guerbet coupling over mixed oxide catalysts. Reproduced from Makoye et al. (2025), Catalysts 15, 8, 709. Licensed under CC BY 4.0. [34]

2. Basis for This Master's Thesis

This work builds on the foundation of prior studies, particularly those demonstrating the promise of MOF-based heterogeneous catalysts [19] [25]. Dahao et al. [19] reported ~50% ethanol conversion and ~50% n-butanol selectivity over a 200 hours continuous test using Pd@UiO-66, where confined Pd nanoparticles and Zr Lewis acid sites show a synergic effect without the harsh pressures typical of oxides. Unlike traditional mixed oxides or HAP, which require extreme temperatures (up to 580°C) and suffer rapid deactivation [28] [30], this MOF approach achieves comparable performance at 250°C and 2 MPa, highlighting its potential for industrial scalability. Our experiments extend this by impregnating UiO-66 with Pd and Cu co-catalysts, testing with different inert materials for the dilution of the catalyst and investigating the effect of different impregnation methods, achieving 33–39% conversion and 27% average selectivity over 60 h in a gas-phase continuous fixed-bed reactor—values that, while lower than batch homogeneous benchmarks [26], demonstrate improved stability and milder conditions relative to other heterogeneous systems [18] [31].

A key motivation for this work is addressing gaps in catalyst stability and deactivation during the Guerbet reaction, as these directly impact selectivity and activity in continuous processes—issues highlighted in our experiments with UiO-66-based systems. While the reaction mechanism remains debated, with key pathways including acetaldehyde self-condensation and ethanol-acetaldehyde direct coupling (as shown in Figure 2), our focus is on how these steps are influenced by practical factors like impregnation methods and metal loading. In the self-condensation pathway, ethanol dehydrogenates to acetaldehyde on metal sites (e.g., Pd), followed by aldol coupling on Lewis' acid-base pairs (e.g., Zr^{4+}-O^{2-}), dehydration to crotonaldehyde, and hydrogenation, potentially via MPV or spillover [19] [33] [28]. Our results reveal that deactivation—linked to acetaldehyde polycondensation, water effects, or Pd coalescence (as seen in TEM post-reaction, figure 11 of section 5.1)—alters these steps, with higher thermal stability (from TGA) correlating to sustained conversion (33–39% over 60 h) and selectivity toward n-butanol.

Essential catalytic properties observed in our study include:

- Activity toward dehydrogenation/hydrogenation, enhanced by Pd loading (optimal at 4%) and Cu co-impregnation for longer-chain products (e.g., n-hexanol, 2-ethylhexan-1-ol).
- Lewis' acid/weak base pairs (Zr^{4+} with O^{2-}/μ_1-OH) to stabilize enolates and favour condensation, as TPD-NH3 and DRIFTS showed Pd reducing strong acid sites while preserving overall synergy [19] [25].

We chose UiO-66 impregnated with Pd/Cu because the MOF's tunable defects and Zr sites provide inherent Lewis' acidity, while Pd/Cu improve hydrogen activation and chain growth under mild conditions (250°C, 2.16 MPa). This addresses literature gaps by investigating water-based impregnation (against n-hexane impregnation), inert dilution (silica gel stabilizing via water adsorption), and bimetallic effects in a continuous fixed-bed reactor, revealing deactivation mitigated by structure and revealing paths for scalable SAF production.

3. Scope

The scope of this research is to explore the potential of Pd impregnated on UiO-66 as a catalyst for continuous upgrading of ethanol to n-butanol, in terms of conversion of the feed and selectivity towards the desired product. Our main goals were to:

- Investigate how the structural stability of the catalysts influenced the catalytic performance;
- Understand how the palladium loading and dispersion affects the activity of the catalyst;
- Assess how the impregnation method affects the selectivity of the catalyst;
- Analyse the evolution of the selectivity of the products under deactivation in reaction conditions;
- Identify the deactivation mechanisms and understand their magnitude;
- Observe the effect of inert materials used to dilute the catalyst on the catalytic performances;
- Investigate how impregnating with different metals affects the selectivity of the reaction.

Other objectives were to observe how the Lewis' acid properties are affected by the co-catalyst and how the activation and reduction steps affect the MOFs. The hypotheses at the base of our research are:

- Activity of the catalyst is dependent on the acid Zr^{4+} and on the Pd particles that activates the hydrogen, the determining step being aldolic condensation [19];
- Deactivation takes place due to mobility of Pd particles that tends to coalesce on the surface reducing the dispersion and specific area along with active sites.

We wanted to produce a catalyst exhibiting good conversion rates (>50 $mmol*h^{-1}*g\ catalyst^{-1}$), good selectivity towards our target molecule (>30%) and able to maintain more than 80% of its activity over 60 hours. While we were able to reach our targets regarding conversion rate and stability, the results regarding selectivity appear to be on the lower side of our >30% target.

4. Materials and Methods

1. Catalyst preparation

The catalyst was prepared following the procedure reported by Pedro Cantarero Gómez et al. [25] under hydrothermal conditions at 120 °C during 24h, the synthesis was carried out in a 250 mL Pyrex reaction vessel. In order to obtain a linker defective material, the conditions reported by Garibay et al. [35] were used, and the synthesis was modulated with benzoic acid. As per the procedure 1.16g of $ZnCl_4$ were added to the reaction vessel and dissolved in 45 mL of NN-Dimethyl formamide (from now on DMF) at room temperature. Then 56.50 mmol of benzoic acid were added to the vessel. In a different glass beaker 4.80 mmol of terephthalic acid were added and dissolved in 45 mL of DMF. The two solutions were then mixed under stirring in the reaction vessel, then moved into a preheated oven at 120 °C for 24 h. Afterwards the solution was allowed to cool to room temperature, the precipitated MOF was then separated by centrifugation. The filtrate was then washed three times over two days using 30 mL of DMF to remove leftover precursors, then the same washing procedure was repeated using methanol to remove any leftover DMF. The product was then air-dried at 80 °C for 12 h to evaporate the methanol.

To impregnate the co-catalyst on the MOF, 500 mg of the catalyst were weighted and added to a 100 mL autoclave bottle along with 25 mL of distilled water, after that the bottle was closed and placed in an ultrasound bath for 10 minutes to break the chunks of MOF. The bottles were then removed from the ultrasound, a magnetic stirrer was added to them and they were placed on stirring plates to stir at room temperature. During the stirring the solutions containing the metal were added dropwise in different amounts depending on the desired amount of co-catalyst. The impregnations were carried out mainly using palladium, in a few tests copper was paired with it. For the palladium solution $Pd(NO_3)_2$ was used to prepare a solution circa 0.1875 M, for the copper $Cu(CH_3COO)_2$ was used to prepare a solution circa 0.062 M. If both metals were desired in the MOF the solution of copper was added first. The samples were then left to stir at room temperature for 20h. The following day the solutions were poured in 50 mL Falcon vials then centrifugated to decant the solids and the liquid was taken out.

Then 30 mL of distilled water were added to each vial, and the vials were manually shaken for 5 minutes then centrifugated again. This process was repeated one more time after which the solids were transferred back in their autoclave bottles alongside 30 mL more of water to stir for 6 more hours at room temperature. Then a further centrifugation and washing were carried out and after pouring everything in the bottles the samples were left to stir overnight. After this the samples were centrifugated and washed 2 more times. After a third centrifugation the samples were put in a preheated 80 °C oven to dry. Once dried the samples were put in a mortar, gently crushed to a fine powder and weighted.

It is important to mention that, some of the impregnations were carried out using the exact same method described above with the only difference that the MOF was being dispersed in n-hexane rather than water.

2. Characterization techniques

After the synthesis the catalysts were tested through XRD to check the characteristic peaks. Another XRD was carried out after the impregnation procedure. XRD characterization shows diffraction peaks based on the crystalline structure of the samples by shining it with an X-ray source and detecting the diffracted radiation at different angles. This analysis was used to check the structure of the catalysts after synthesis and reduction processes.

ICP analysis was carried out to check the amount of co-catalyst that was impregnated on the MOF. ICP analysis allows a quantitative and qualitative response to the metal atoms present in the sample. By using this test, we were able to quantify the amount of palladium present in our catalyst.

Scanning TEM analysis was carried out on a catalyst to observe how the palladium dispersion was affected by the reduction process and during the reaction.

XPS analysis was carried out to observe which palladium species were present on the sample after the reduction step and if palladium was present on the surface of the catalyst.

XPS, TEM, XRD and ICP analyses were carried out by external laboratories.

TGA analysis was carried out to check the thermal stability of the catalyst. We tested the samples after the impregnation process to observe how their structure behaved at high temperatures and if the impregnation procedure affected the stability of the catalysts. The analyses were carried out in an air-like atmosphere (20% oxygen, 80% nitrogen), using a ramp of 7K/min, starting from 35°C up to 900°C.

TPD analysis was used to assess the amount and strengths of the acid sites present in the MOFs. The TPD was carried out by cleaning the quartz tube, adding some quartz wool at the bottom and weighting it, afterwards the sample was added in the tube with the help of a funnel, the tube was then weighted again to calculate the sample mass, then another piece of quartz wool was added on top of the sample. The tube was then placed in the machine and the analysis started. First the machine checks the flow through the tube to ensure that the sample and the wool aren't to compact, then the analysis starts and a mixture of NH_3/He (10% v/v) is passed through the tube to allow the adsorption of the ammonia. The tube is then flushed with He to remove the excess ammonia, the analysis then starts by heating up the sample and measuring how much ammonia exits the tube by means of a TCD detector. We compared data between different catalysts with different palladium amounts to see their differences. We used a ramp of 10°C/min up to 270°C. The MOFs were pretreated in a reducing atmosphere of 10% H_2/N_2 at 270°C for two hours before using them in the TPD test.

Other tests carried out on the catalysts were DRIFTS to observe how the various peaks changed during the processes carried out on the catalyst. The pattern obtained shows the evolution of the peaks after processing our catalysts. Specifically, we observe how the peaks relative to the OH groups shifted and if the MOF structure suffered transformations during the reduction step. The measurements were carried out at room temperature, in a nitrogen atmosphere and the samples didn't undergo any sort of pretreatment except when stated otherwise.

3. Reactor Setup and Conditions

The reaction setup included: a tubular inox steel reactor with a vertical furnace for heating, various heating belts to keep the lines at a temperature high enough to avoid condensation, an in-line GC-FID to check the products during the reaction and a bubbler at the outlet of the GC to condense some of the heavier products as well as to allow to see the flow of the gases through the reactor, the vessel holding the ethanol and a helium tank to pressurise the ethanol and push it in the reactor. The temperature in the reactor was controlled by a thermocouple fixed in the middle of the catalytic bed and the heating was adjusted by PID controllers. All the flows for the gases and ethanol were modulated by mass flow controllers. The whole setup was placed inside of a fume hood. A small amount of glass wool was added at the internal extremities of the reactor and was kept in place by a piece of steel mesh, this was to stop any catalyst from leaving the reactor, afterwards the tube was filled with coarse SiC, then fine SiC, then some more fine SiC with the MOF mixed in, another layer of fine SiC and finally a last layer of coarse SiC. The reactor was then closed, connected to the plant and checked for leaks by slowly pressuring it until 2.5 MPa with nitrogen, if after 10 minutes the pressure didn't change the reactor was considered sealed and we would continue with the next step after slowly bringing the pressure back to ambient. The reactor was then flushed with N_2 during the heating phase, then after reaching the setpoint the gas flow was changed to a mixture of 10% by volume H_2/N_2 for 2 hours at 270 °C allowing the palladium salt to get reduced. After that, a cooling phase to temperature condition (250 °C) was set with N_2 flow, and a pressurization phase followed, reaching and 2.16 MPa. At this point the ethanol started flowing along with N_2, the WHSV was 8,5 h^{-1} ($\frac{g/h\ of\ ethanol}{g\ of\ catalyst}$). After an initial "lag phase" during which the nitrogen was progressively being flushed out by the ethanol + nitrogen inlet, the atmosphere composition inside the reactor became constant and we reach the stationary condition. The lag phase lasted approximately 5 hours.

4. Product Analysis

The products were carried out of the reactor through a steel line heated by means of a mantle connected to a power regulator, the line was kept at 180 °C

which was checked before and during every reaction by means of a thermocouple, the outlet line was at room pressure and it was directly connected to the GC 6-way valve which was also heated to 200 °C, the loop was continuously filled with the mixture of products and every 22 minutes an injection was executed. The opening of the valve lasted 24 seconds in order to allow the loop to be completely flushed by the carrier (Ar), the temperature program was set to keep the temperature at 50°C for the first 4 minutes, then increasing it by 10°C/minute for 12 more minutes, the remaining 6 minutes were needed to cool the column and make sure the temperature was stable. Over the 6 months of tests, we had problems with the 6-way valve, some dark carbonaceous residue would clog the line stopping gas flow. This was likely due to polymerization of the acetaldehyde which was among the most abundant products, this happened only a couple of times and it was, apparently, not related with catalysts showing high activity. The retention times were identified by means of manually injecting commercial chemicals into the column of the GC after diluting them in other solvents, first the main known products of the Guerbet pathway were injected, then over the months we tried identifying other major peaks by injecting other possible products such as ethane (dehydration of ethanol and successive reduction) and 1-hexanol. We tested molecules that were reported on other similar works that operated in the framework of Guerbet reaction catalysed by heterogeneous catalysts, mostly linear products but also some branched products that appeared in very small amounts in some tests. Some blanks of the reactor filled with the inert were carried out in order to be sure that no significant catalytic activity was due to the SiC or the inox steel that made up the reactor. These tests showed that the conversion due to the silicium carbide and the reactor wall is negligible.

5. Results

1. Characterization

The XRD analysis shows the crystallographic peaks of out MOF structure, after impregnation (red) and after the reduction step (purple). We can see how after the reduction step specific peaks associated with metallic palladium appear.

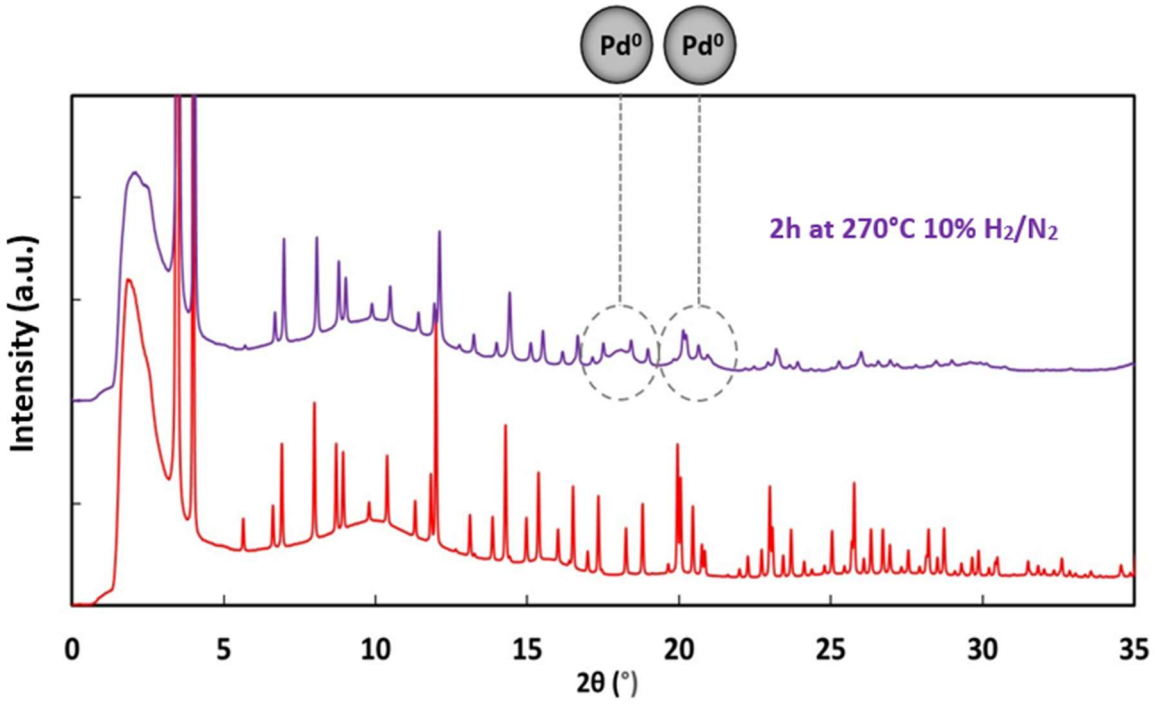

Figure 4 XRD of the catalyst after the impregnation (red) and after reduction (purple)

We can see the structure of the MOF remaining intact after the reduction process, indicating the stability of the catalyst at reduction conditions. Specific peaks of metallic Pd also appeared, indicating the successful reduction of the palladium salt along with the formation of crystallites of palladium metal.

The ICP confirmed that the real amounts of Pd impregnated in the catalyst is extremely close to the theoretical amount.

The TGAs showed differences in the first decomposition peak of up to 70°C for some catalysts. In figure 5 we can observe the decomposition of two catalysts, the mass lost at the beginning of the analysis is associated with adsorbed water, while the mass lost around 400°C is associated with benzoic acid (used during the synthesis to produce defect/missing linker sites) and linker degradation.

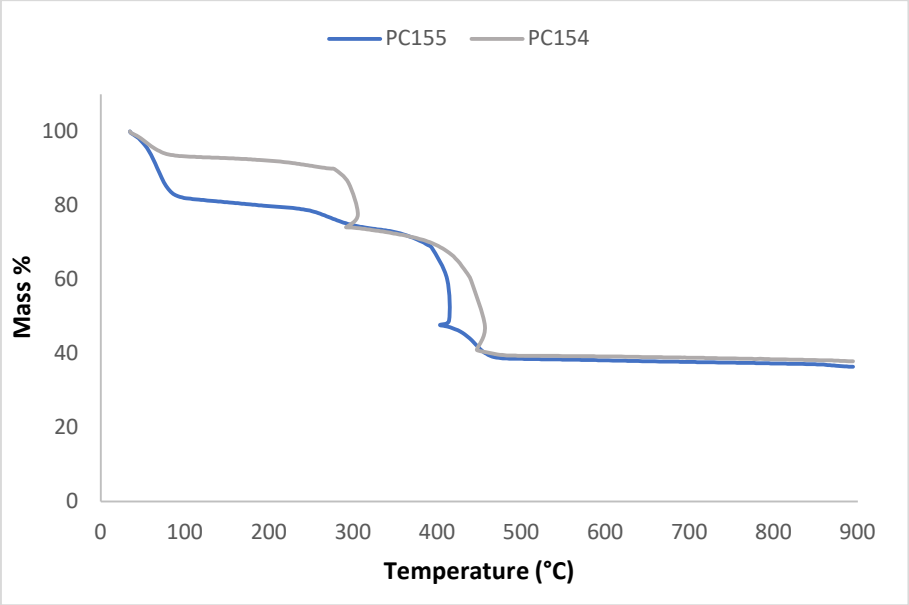

Figure 5 TGAs of two catalysts with different Pd content (4% Pd indicated by the blue line, 1% Pd indicated by the grey line) showing significant differences in the first decomposition temperature

We observe two clearly different behaviours between these two catalysts, PC155 shows a curve coherent with what Cantarero et Al. observed during their research while PC154 exhibits an anomalous decomposition curve.

The DRIFTS spectre shows peaks relative to the organic linkers in the structure that are kept after the reduction step (orange curve). The catalyst before the redaction step (blue curve) exhibits a wide peak in the 2600-3700 cm^{-1} region that is associated to adsorbed water.

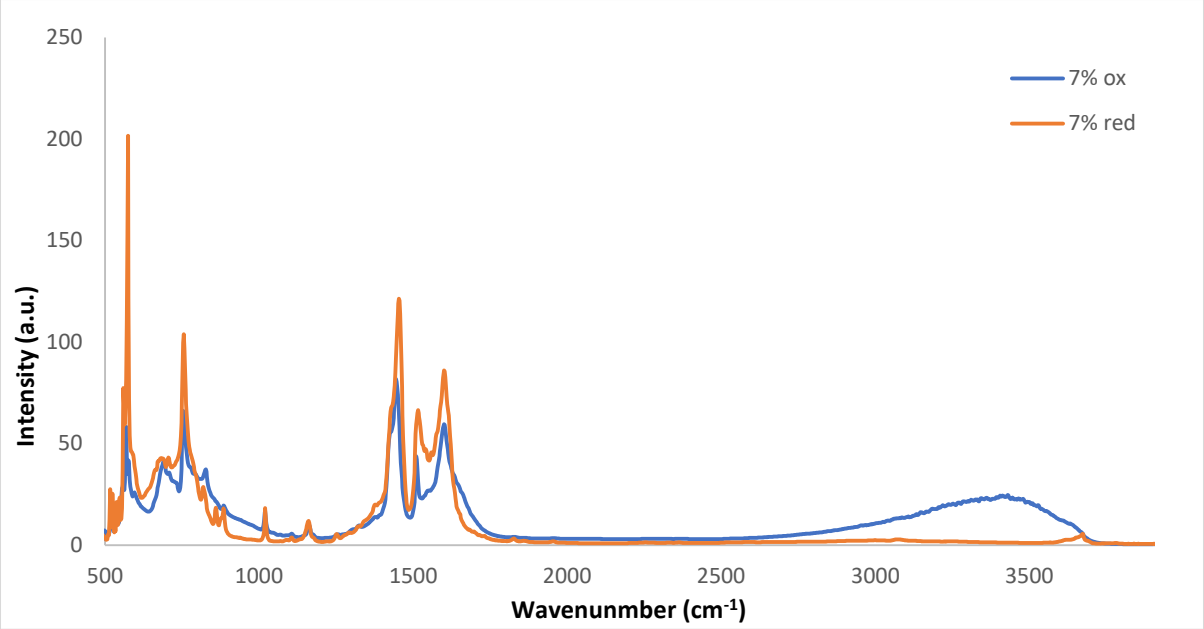

Figure 6 DRIFTS of a catalyst before (blue) and after (orange) the reduction treatment carried out at 270 °C for 2h in an atmosphere of 10% hydrogen in nitrogen.

We can see from figure 6 that the peaks associated with the organic structure of the MOF don't undergo any significant change during the reduction process, indicating the structure stability at reduction conditions confirming what we observed with XRD analysis. The changes in the wide peak between 2600 and 3700 cm^{-1} are due to loss of water that was absorbed in the MOF, which makes sense as the reduction pretreatment is carried out at 270°C which is a high enough temperature to remove all of the water present in the sample.

Figure 7 shows a detail of the region in which we are able to see OH groups associated with the missing linker site shown in figure 9. Specifically, the three peaks present in the 0.5% sample (grey curve) at 3630 and 3674 cm^{-1} are associated with isolated μ3-OH groups. While the μ1-OH group should appear at 3780 cm^{-1} but it is not present after the pretreatment at 120°C following the impregnation.

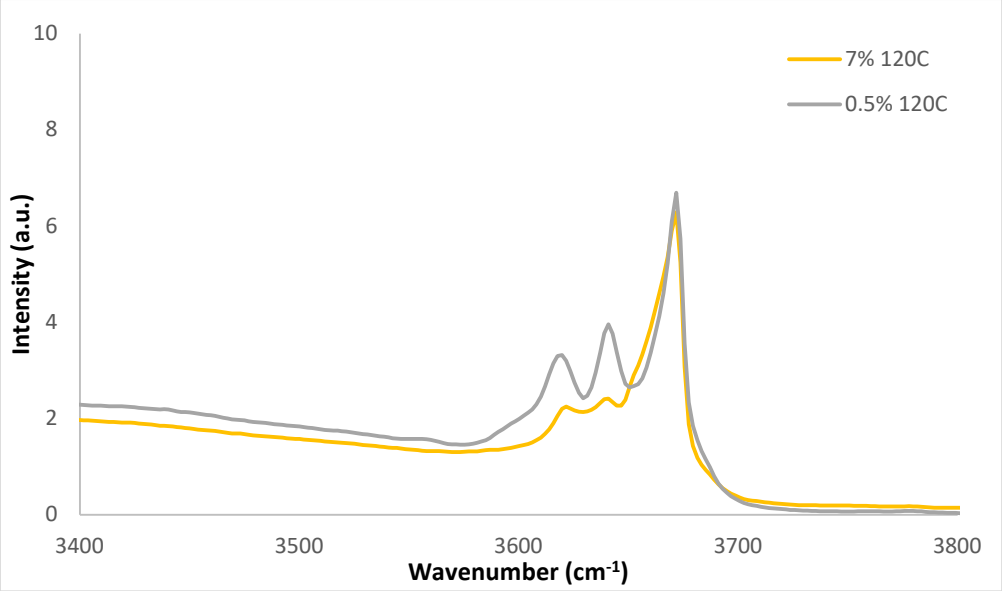

Figure 7 DRIFTS spectra of two catalysts sample with diffent Pd loading after a pretreatment at 120 °C to remove leftover water and show characteristic peaks of OH groups

In the figure above we can see the characteristic peaks of the OH groups left on the Zr atoms thanks to the modulator, in the catalyst with the lower loading the peaks are more intense showing a higher amount of OH groups while in the catalyst with the higher loading the peaks are greatly reduced in intensity. The peaks that lost intensity are related to μ3-OH groups as well as tallest peak to the right [25]. This indicates that the impregnation procedure is selectively affecting the some of the μ3-OH present in the structure on the missing linker site. Cantarero et Al. [25] highlight the importance of the μ1-OH groups that show up at 3780 cm^{-1} which do not appear in these sample after impregnation and pretreatment to remove adsorbed water. These results indicate that the impregnation and grafting of the palladium depends on the presence of these OH groups.

In figure 8 we can see the same region of figure 7, this time after the reduction process was carried out on two catalysts samples. After the reduction step the peak associated with μ1-OH groups is clearly visible, although is much more evident in the 4% palladium sample (yellow) rather than in the 7% palladium (orange).

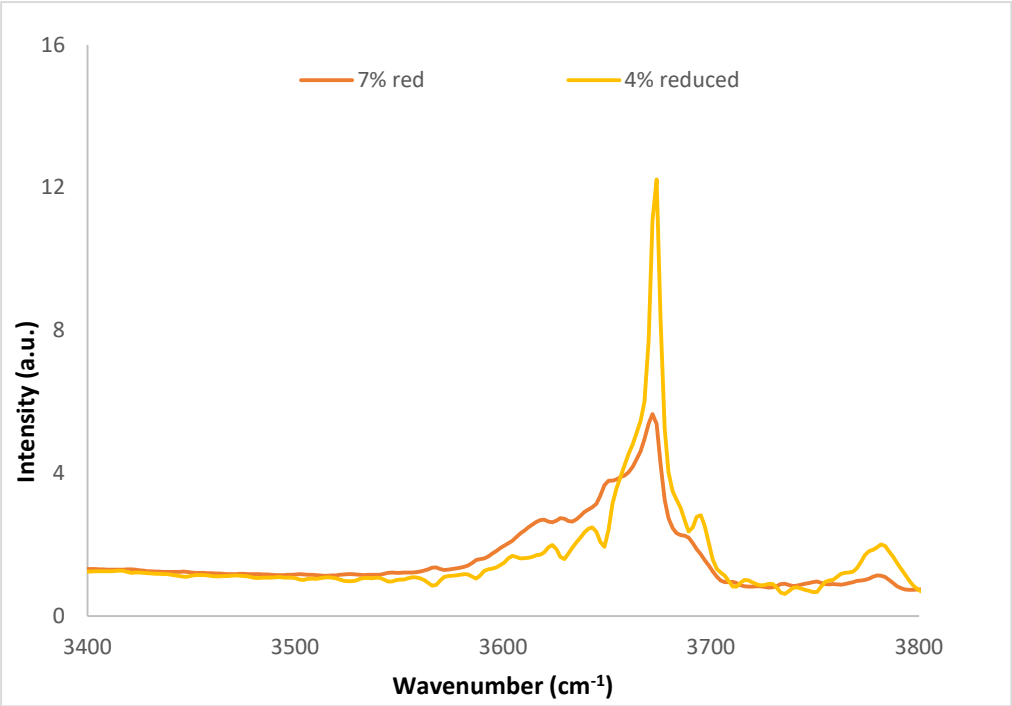

Figure 8 DRIFTS spectra of two catalysts sample with different palladium loading after the reduction step, showing the peak associated with μ1-OH groups.

After the reduction pretreatment we can see how μ1-OH specific peak is present in our catalyst in accordance to the observation of Cantarero et Al. [25].

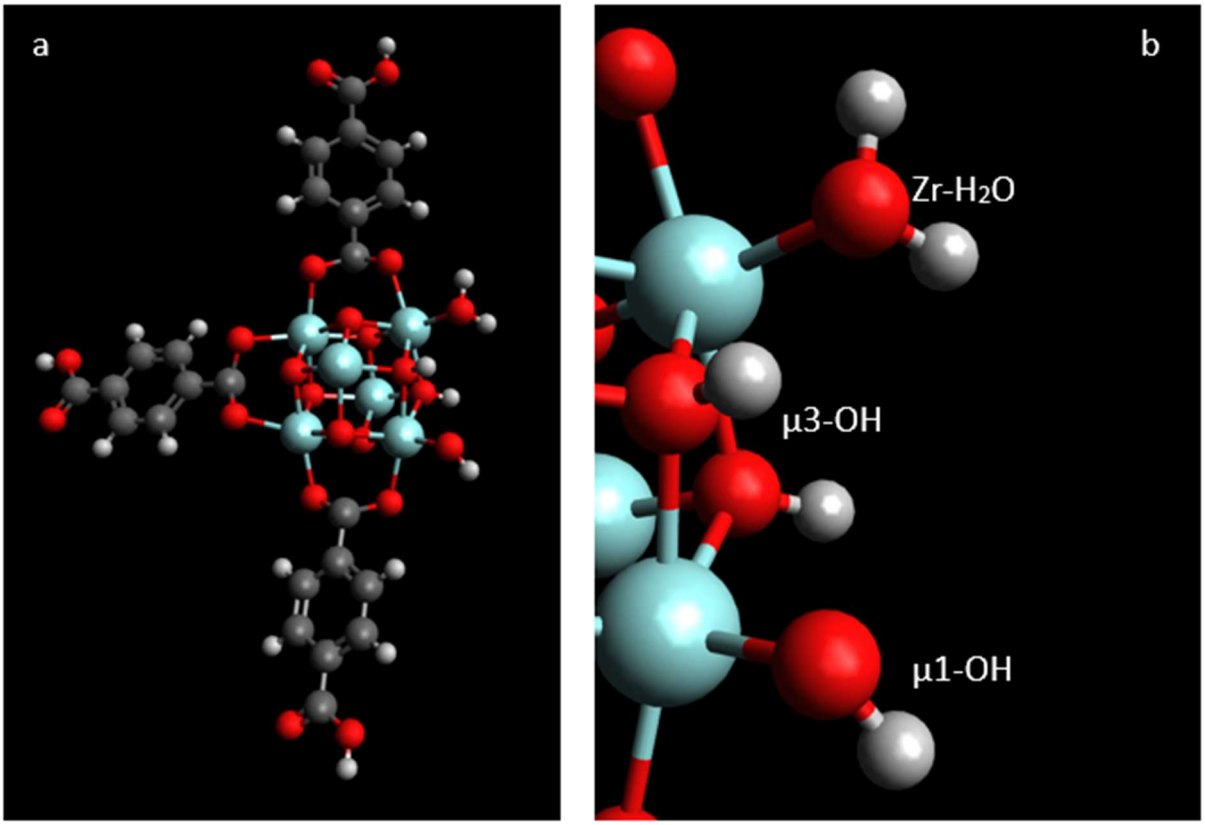

Figure 9 structure of Uio-66 unit (a) with a missing linker, where light blue atoms are Zr, red are O, dark grey C and light grey H; detail of the acidic hydrogens present on a missing linker site (b);

The TPD represented in figure 10 shows the desorption rate of two catalysts with different palladium loading to compare the amount and strength of their respective Lewis' acid sites.

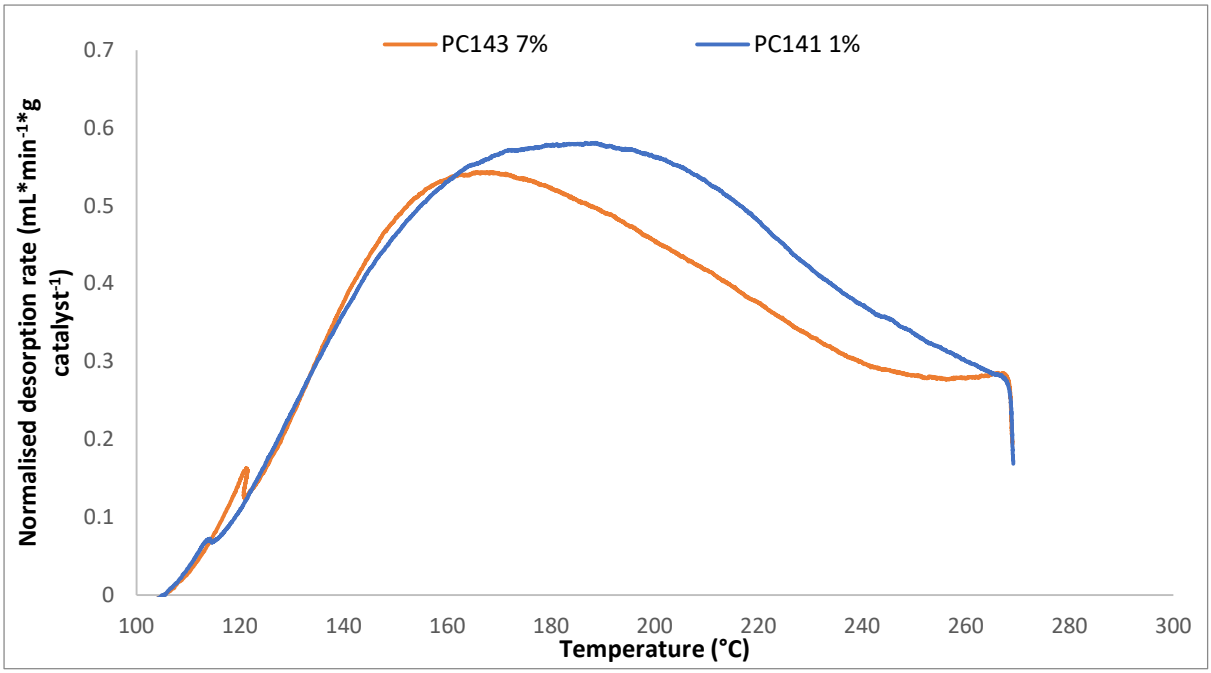

Figure 10 TPD-NH3 of two samples of Uio-66 with different amount of Pd loading, 7% Pd (orange) and 1% Pd (blue)

We can see how in figure 10 the stronger acids sites appear less abundant in the catalyst with the higher palladium loading (orange 7% palladium), while the weaker ones appear to be less affected. This suggests that palladium is blocking stronger Lewis' acid sites, as a higher metal loading is associated with a smaller desorption rate at higher temperatures.

The XPS analysis was carried out in an external laboratory using a SPECS system (Berlin, Germany) coupled with a Phoibos 1D-DLD detector and a monochromatic source Al Kαα (1486.7 eV).

PC106_4 Pd_después reacción							
Cycle	Name	Position	FWHM	R.S.F.	Area	% Conc.	% Atomic rel
C	C 1s	284.6	3.515	1	25100.7	55.557	55.6
O	O 1s	530.4	3.847	2.93	40767.1	30.796	30.8
Zr	Zr 3d	183.4	4.438	7.04	27313.2	8.587	8.6
Pd	Pd (3d 5/2), red	334.7	3.645	16	19491.9	2.696	4.5
	Pd (3d 3/2), red	340.0	3.386	16	13073.7	1.809	
*Cl**	*Cl 2s*	269.0	4.7	1.69	423.6	0.555	*0.6*
* *Espectro cercano al ruido, estimación*							

Table 2 showing the results of the XPS analysis

The XPS analysis highlighted that the only type of palladium present on the catalyst surface after the reduction is associated with metallic palladium confirming the effectiveness of the reduction step in reducing the metal.

Some post-characterizations with STEM-HAADF were able to show the inorganic MOF structure (blue) and the palladium particles present on it (red).

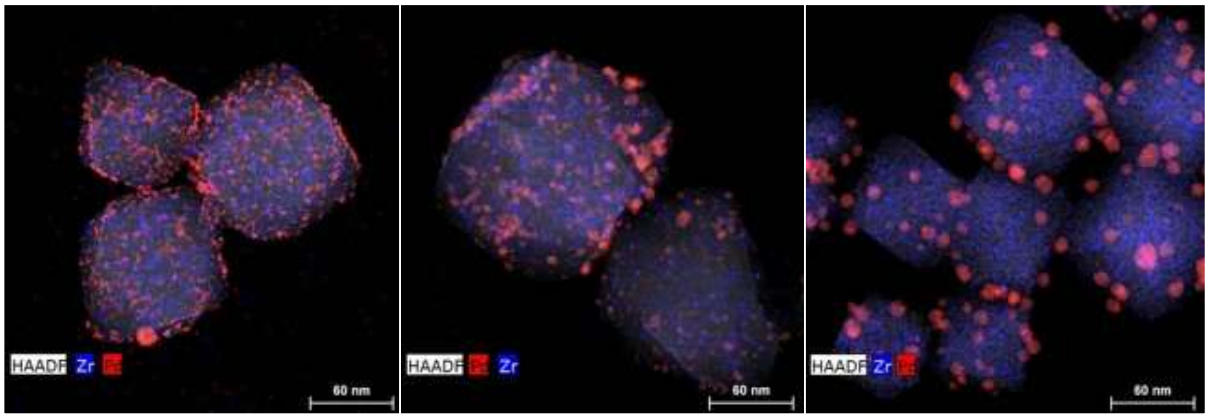

Figure 11 show a STEM-HAADF of a 4%Pd catalyst after drying (a), reduction at 270°C for 2 hours in 10% hydrogen/nitrogen mixture (b) and after 15 hours of reaction (c)

We can see that after the reduction some Pd particles already started coalescing but we can still see many small ones dispersed over the catalyst, this confirms the observations made with XRD that showed palladium-specific peaks. After 15 hours of reaction almost all of the smaller particles disappeared. The coalescence of the palladium particles reduces its surface area and number of active sites associated with it. This phenomenon could be responsible for the deactivation that we observed during the catalytic testing of the MOFs, the change in the conversion rate showed in figure 13 highlights deactivation of catalysts during the reaction.

2. Catalytic Activity

1. Effect of thermal stability on catalytic performance

Many catalysts showed promising results of conversion and selectivity towards the 1-butanol. Other linear alcohols were detected in smaller quantities such as 1-hexanol. The activity of the catalyst wasn't always directly correlated with the Pd loading but it was always correlated with the thermal stability. For example, the catalysts PC142 and PC155 (both impregnated in n-hexane and loaded with 4% palladium) showed different thermal stabilities and very different conversion rates.

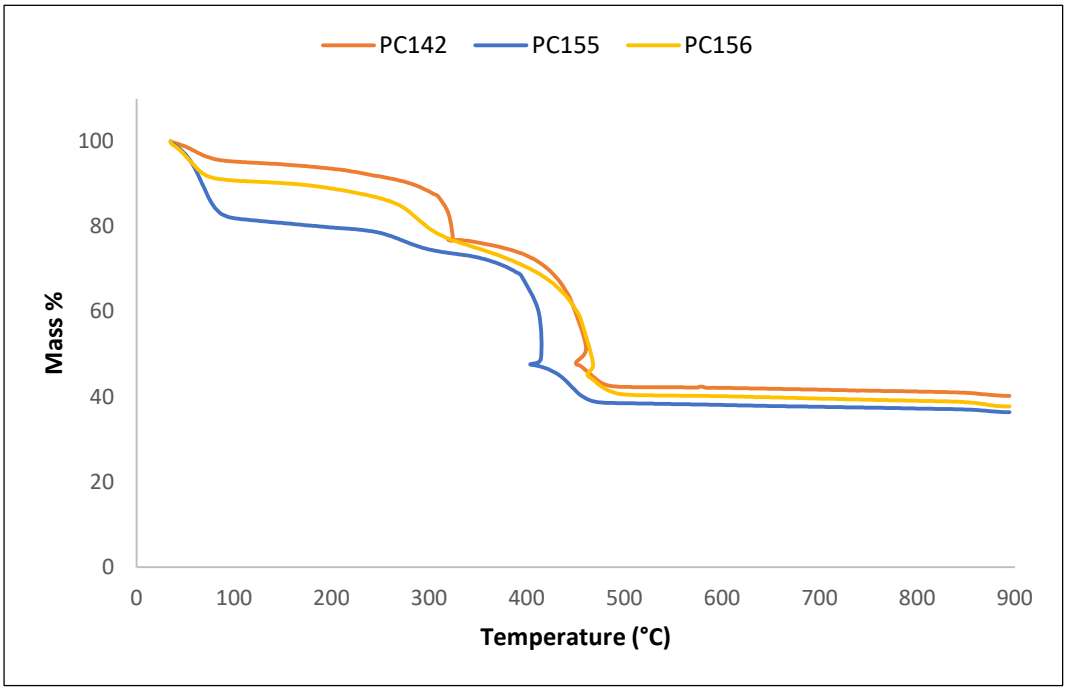

Figure 12 TGAs of three catalysts, PC155 and PC142 are loaded with the same amount of Pd (4%) while PC156 has a higher loading (7%)

We can see in the figure above that the TGAs between the three catalysts appear to be quite different as PC142 shows two clear peaks, the first one at 310°C and the second one at 429°C. Both of these peaks correspond to an exothermic decomposition, PC155 shows a first mass loss at the beginning of the analysis that corresponds to adsorbed water and then only shows one decomposition peak at 395°C. Both of these catalysts were impregnated using the same method but showed a significant difference in thermal stability. PC156 exhibits a slower decomposition compared to PC142, indicated by the slope of its curve, starting at 300°C and then a second decomposition at around 429°C. This indicates that the impregnation process can have some

detrimental effects on the structure, which translates to a reduced thermal stability. This effect appears to be independent of palladium loading.

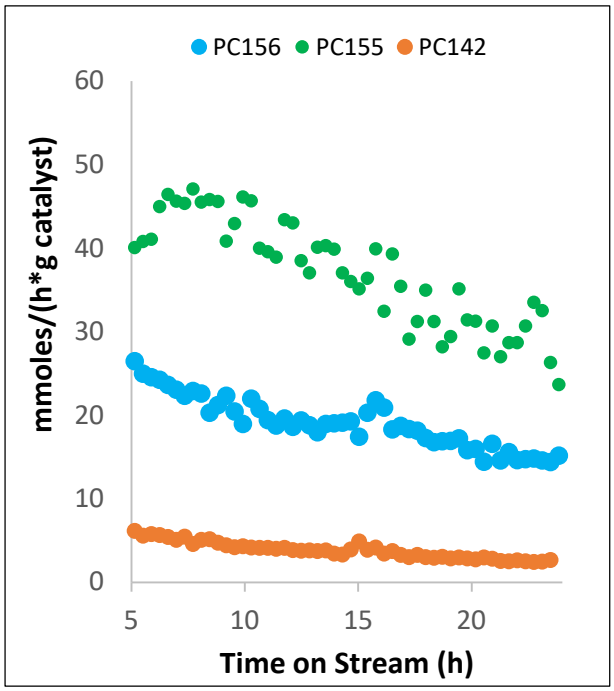

Figure 13 Graph comparing the conversion rates of the feed of three catalysts (palladium content is4% for PC155 and PC142 and 7% for PC156); tests were carried out in the same conditions, 2.16 MPa, 250°C and with a WHSV of 8.5 h^{-1}, the amount of catalyst loaded in the reactor was 82 mg

Figure 11 shows that PC155 is almost 5 times as effective as PC142 in converting the feed, but at the same time it shows that PC155 is deactivating faster than PC142. We can observe the deactivation rate based on the slope of the data series, PC155 has a greater slope than PC142 meaning that it is deactivating faster. This is also true for PC156 which exhibits a higher activity than PC142 but lower than PC155 and a slower deactivation rate than PC155 but higher than PC142. This result shows that deactivation rate and product conversion have a connection between them, as a higher conversion rate corresponds to a higher the deactivation rate. Since PC155 showed a greater thermal stability, we can say that the predominant deactivation mechanism is not dependent on the temperature, otherwise we would observe a faster deactivation in PC142 and PC156 rather than PC155. As for the products, PC142 only shows a few: ethylene, ethane, acetaldehyde, n-butanol and crotyl alcohol. PC155 on the other hand showed all the products of PC142 and others such as n-hexanol, 2-ethylhexan-1-ol, butanal and crotonaldehyde. We can also observe some interesting trends in the selectivity/conversion graphs that are following.

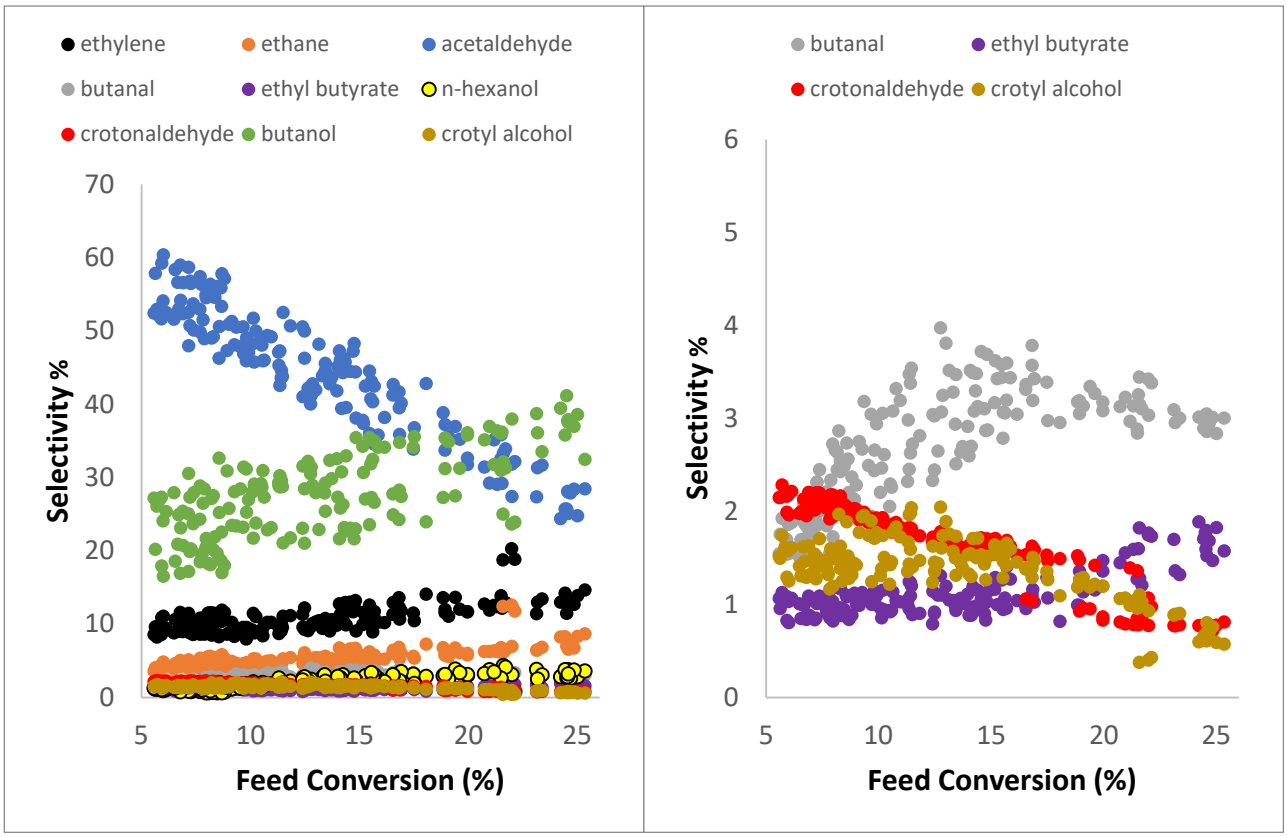

Figure 14 selectivity/conversion graphs of PC155

We can observe how in the left of figure 12 the trends of the major products (acetaldehyde, n-butanol, ethylene and ethane) are linear, meaning that all of these products are primary products coming from ethanol. The major products are acetaldehyde and n-butanol, and we can clearly see how the sites responsible for butanol production deactivate rapidly as show by the trend of butanol selectivity. In the right figure we can observe a detail of some minor products, crotyl alcohol and butanal appear to be intermediates. Their downward concavity curve means that when the catalysts id fresh (high conversion) they are transformed into other products. For example, the butanal could either get reduced further to n-butanol or it could form ethyl butyrate through oxidative esterification catalysed by palladium, which would explain its trend. Its upward concavity curve shows that when the catalyst is fresh it is more likely to transform intermediates into this product, but as the conversion decreases (deactivation of active sites) the active sites responsible for the formation of this product deactivate faster. Crotyl alcohol also appear to be an intermediate while crotonaldehyde by comparison appears to be a primary product but it's hard to tell as the trend is not too clear.

The amount of palladium loaded on the catalyst didn't appear to be the main parameter influencing the catalyst activity, rather the thermal stability seems to play a much more crucial role. As we can see from figure 11, where PC156 containing 7% palladium shows lower conversion rates compared to PC155 that only contains 4% palladium. When the thermal stability is comparable like in PC142 and PC156 (figure10) we can see that palladium loading appears to increase the catalyst activity as shown in figure 11. This difference could also be attributed to a slightly higher thermal stability by PC156 as we can observe from the different slope that PC142 and PC156 exhibit after 300°C.

Regarding the selectivity towards n-butanol the highest is shown by PC155, then 156 and last 142. This result shows that a higher activity is related to a higher selectivity towards n-butanol, our target product.

2. Inert effect on catalytic performance

Between the many tests we performed we also tried to mix the catalyst with a different inert to see if it would make a difference, for this reason we tested again PC155 this time mixed with silica gel (calcined at 800°C).

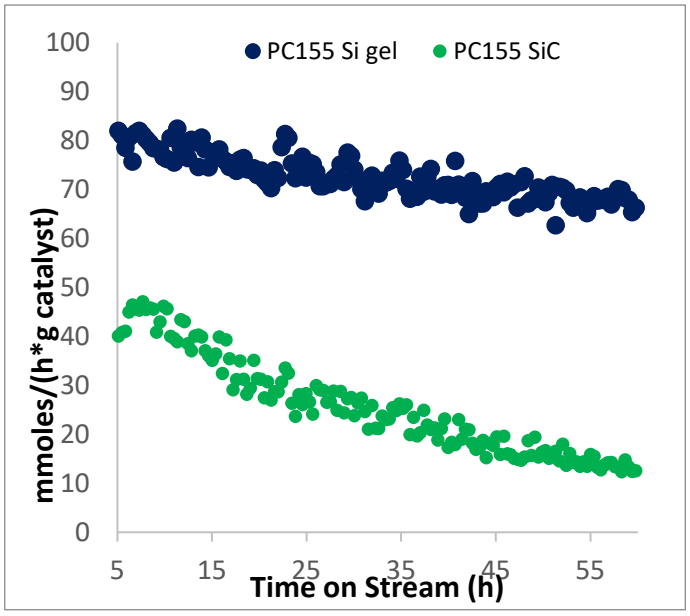

Figure 15 Comparison of conversion rates between two catalysts mixed with silica gel (blue) and SiC (green), the tests were carried out in the same conditions and the amount of catalysts used was 82 mg

We can observe how the conversion rates are quite different between the two tests, this could be due to the silica gel being active towards the reaction, so we carried out a blank test that showed no differences with the one carried out previously with just the SiC in the reactor. This means that there's something more behind the enhanced activity, it could be possible that the catalyst and the silica gel are interacting with each other. We can also observe how the catalyst mixed with the silica is deactivating at a slower rate that the one mixed with SiC. This would also suggest a stabilizing effect by the silica towards the catalyst.

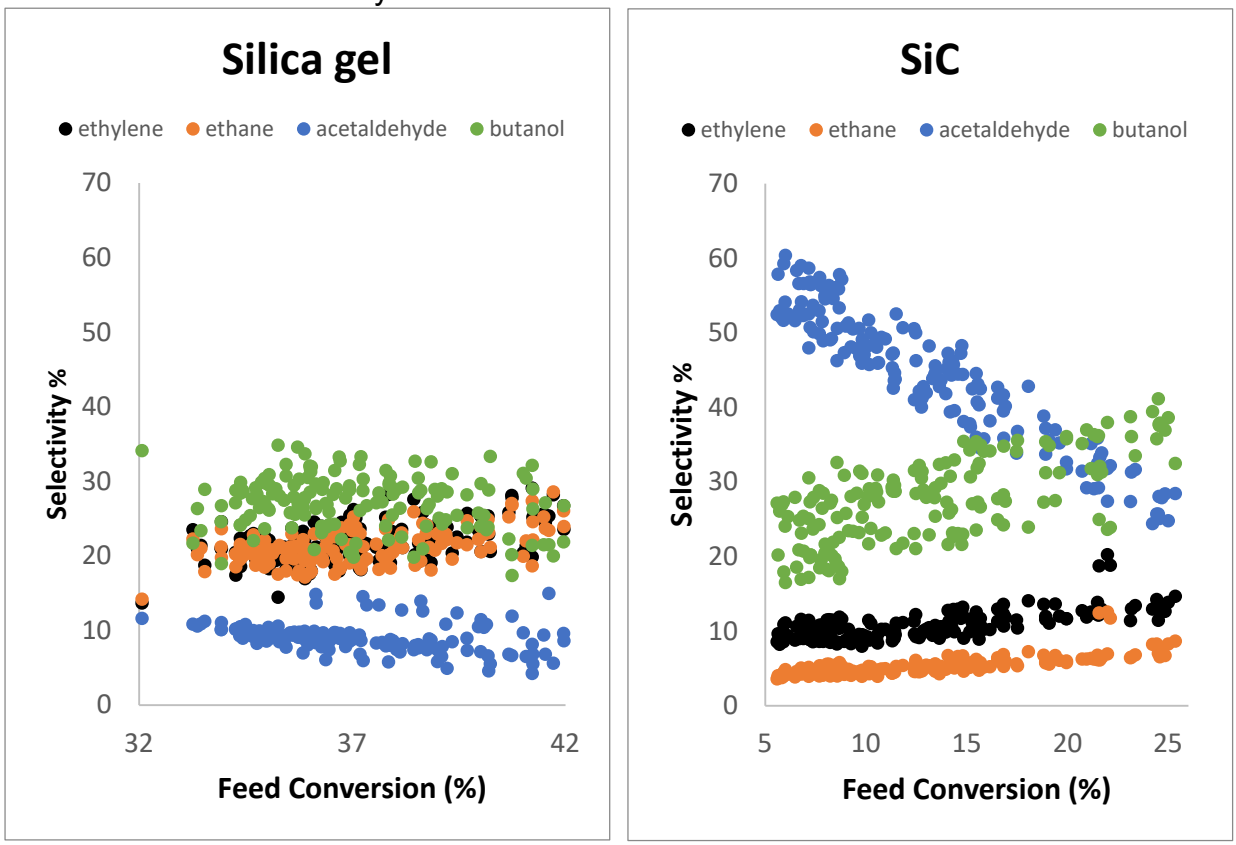

Figure 16 Selectivity/conversion graphs for PC155 with silica gel and SiC for comparison

We can see how the silica gel also affects the selectivity, especially towards acetaldehyde which drops considerably with respect to the catalyst in SiC, while selectivity towards ethylene and ethane is enhanced. This effect on selectivity might be due to SiO_2-related acids site that favour dehydration products, or the water produced during the reaction being adsorbed by the silica shifting the equilibrium. We can observe how with a water adsorbent substance to dilute the catalyst and with a much lower selectivity towards acetaldehyde our catalyst is more stable and more active. The deactivation

might depend on the presence and amount of either water, acetaldehyde or both.

3. Impregnation effect on catalytic performance

We then tested a different impregnation method, instead of suspending the catalyst in n-hexane for the impregnation process we tried suspending it in water, we prepared a 1% Pd-Uio66 and compared to another 1% sample previously tested. PC141 is our catalyst impregnated by suspending it in n-hexane, while PC164 is the one impregnated by water suspension.

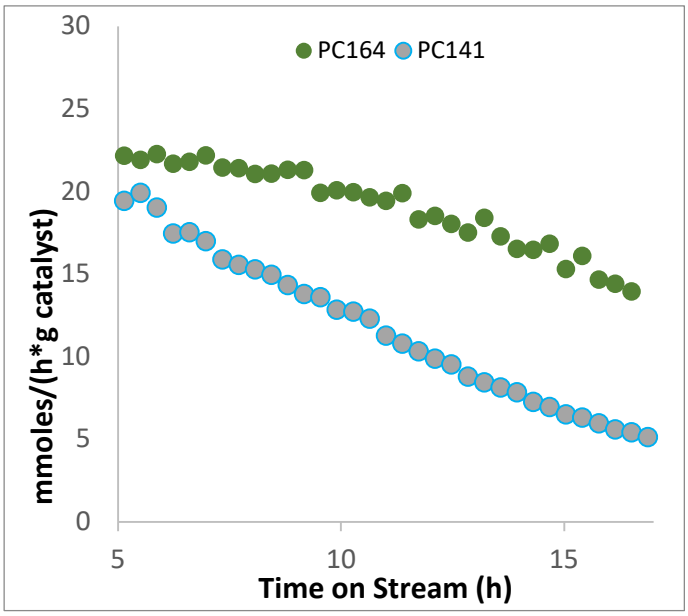

Figure 17 Conversion rates of two catalyst impregnated using different methods; tests were carried out in the same conditions, 2.16 MPa, 250°C and with a WHSV of 8.5 h^{-1}, the amount of catalyst loaded in the reactor was 82 mg

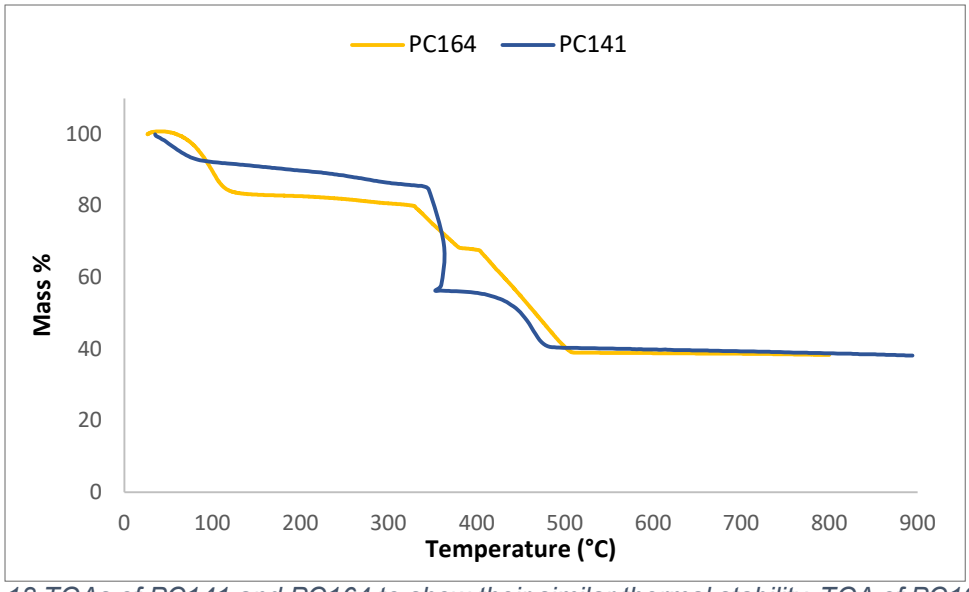

Figure 18 TGAs of PC141 and PC164 to show their similar thermal stability. TGA of PC164 was carried out on a different instrument as the one used for the analysis of PC141 was unusable due to technical issues.

The catalysts exhibited similar thermal stability, although the curves appear to be different this might be due to the two analyses been carried out on different machines. Despite that we can see how both catalysts show a first decomposition peak at around 330°C. Although both catalysts contain the same amount of Pd they show a different conversion rate, specifically PC164 is more active in converting ethanol, more selective towards n-butanol and also showed n-hexanol among its products, although in very small amounts.

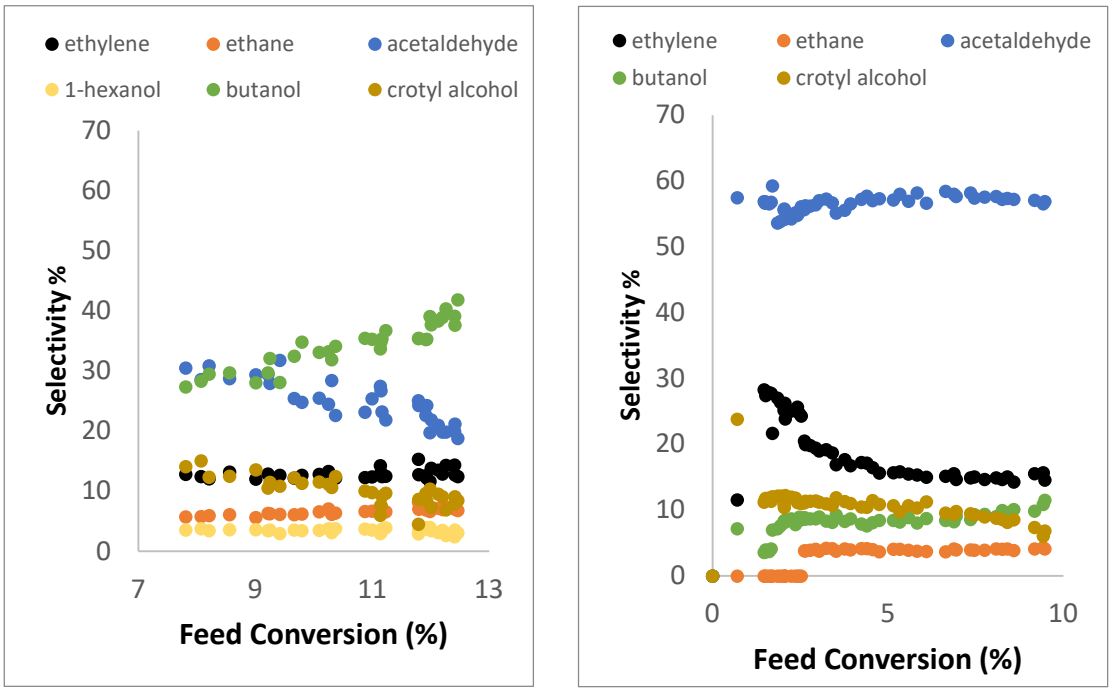

Figure 19 selectivity/conversion graphs of PC164(left) and PC141(right)

PC141 appears to be more selective towards ethylene and acetaldehyde while PC164 produces mainly n-butanol and acetaldehyde. In the figure to the right, we can observe how acetaldehyde shows the highest selectivity, and the catalyst more selective towards acetaldehyde also shows a faster deactivation rate, similar to what we observed with the catalysts loaded with 4% of Pd. This supports the theory that acetaldehyde might be directly involved in the deactivation mechanism. The trends of crotyl alcohol and ethylene show that the active sites responsible for these products are less prone to deactivation than the others, because as the catalyst deactivates their selectivity increases. The figure to the left show trends similar to PC155 (diluted in SiC), except for crotyl alcohol which was barely detectable with the 4%Pd catalyst. We can still see how all the products show a linear trend meaning they are primary. We can observe the selectivity of crotyl alcohol going up as the

catalyst deactivate which indicates that catalysts loaded with 1%Pd possess active sites that are selective towards crotyl alcohol and deactivate slower than other sites. The difference in the other products trend between PC164 and PC141 is likely due to the different impregnation method. Which can also be responsible for the presence of different active sites in the two catalysts.

4. Effect of bimetallic impregnation

Last, we have tested impregnating with two different metals, Pd and Cu, using the water impregnation method, unfortunately the copper didn't attach to the MOF as well as the Pd and during the washing steps the water was always slightly blue. For this specific set of samples, we checked the amounts of metals through XRF to see if the Cu would attach itself to the MOF, but the Pd/Cu ratios measured during testing were off in respect to the theoretical amounts. Palladium attached itself to the MOF in higher amounts with respect to copper. The catalytic activity showed by these catalysts is mostly due to palladium. Despite that we still went through with the catalytic tests to see how they would behave. We tested 1%Cu1%Pd, 4%Cu1%Pd and 1%Cu4%Pd, using the XRF results we were able to estimate the amount of metals.

Theoretical amounts	Real amounts (using XRF Cu/Pd ratio)
PC161 1%Cu 1%Pd	0.07%Cu 1%Pd
PC162 4%Cu 1%Pd	0.22% Cu 1%Pd
PC163 1%Cu 4%Pd	0.06%Cu 4%Pd

Table 3 showing theoretical and real co-catalysts loading in catalysts with mixed metals

Again, the catalysts showing the higher thermal stability also showed the higher activity. These results being observed again in bimetallic impregnated catalysts strengthens the hypothesis that ties the catalyst activity with its thermal stability.

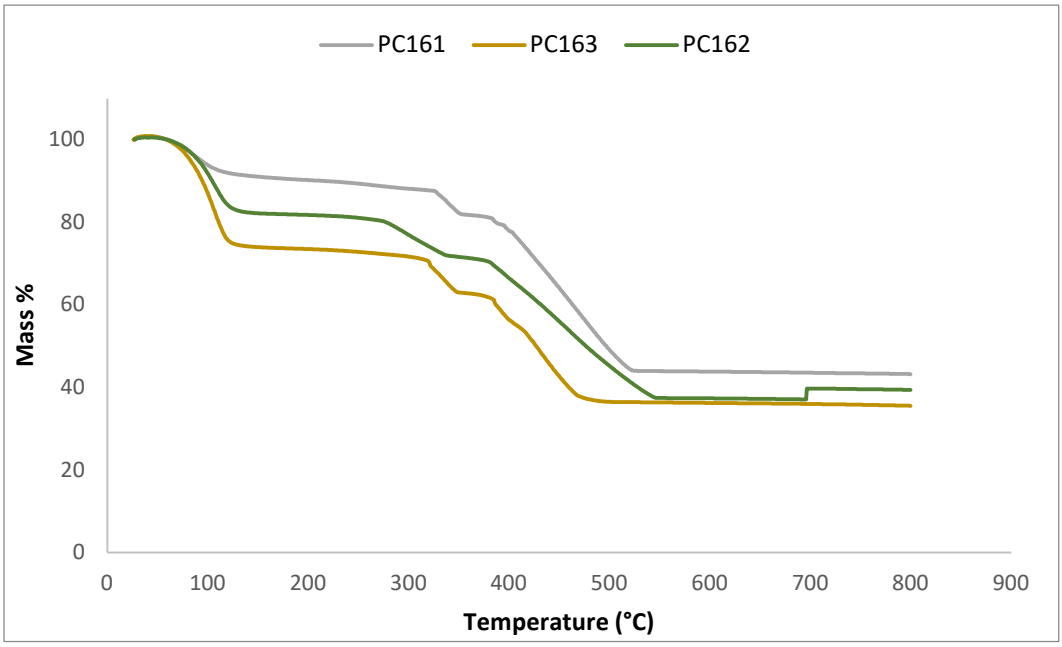

Figure 20 TGAs comparing thermal stability of the three CuPd impregnated catalysts

We can see how the catalysts PC161 and 163 show very similar TGA's curves while PC162 appears slightly less stable at the beginning but it's losing mass slower compared to the others indicating a slower decomposition rate. This could be due to the higher copper content that stabilises the structure, as PC162 has almost 4 times the copper content of the other catalysts.

In these last catalysts we observed a number of substances with elution times higher than 12 minutes (for reference n-hexanol is between 11.36 and 11.48 depending on the width of the peak), these are long chain molecules that we observed in small amounts in Pd impregnated catalysts with high activity (such as PC155) but in this specific case when we tested PC161 and PC163 (the ones that showed the highest conversion rates), we were able to observe significantly more peaks, although very small, at higher times, unfortunately we weren't able to identify this long chain products.

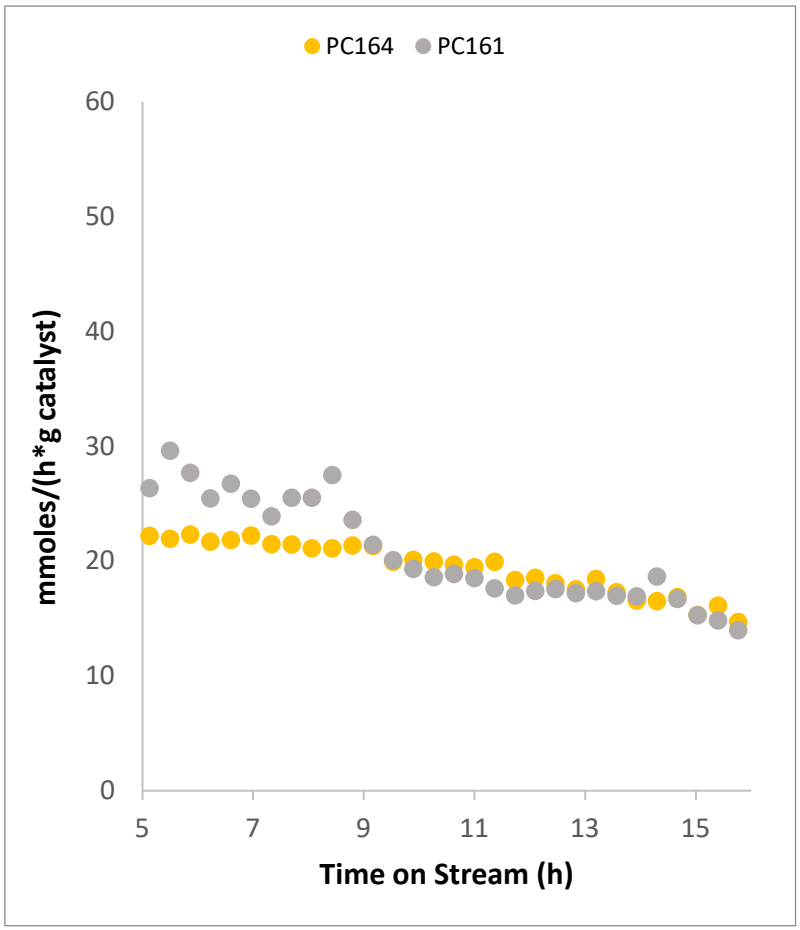

Figure 21 Conversion rates of catalyst PC161 containing CuPd compared with PC164 containing the same amount of Pd metal and impregnated with the same method for comparison

We observe how the conversion rates are almost the same for both catalysts. This indicates that the small amount of copper that is present in PC161 is not affecting the activity. But as stated previously we were able to see different products in the GC peaks, which indicates that despite not affecting the catalyst activity the small amount of copper was enough to affect the chain growth mechanism by increasing the selectivity towards longer chained products.

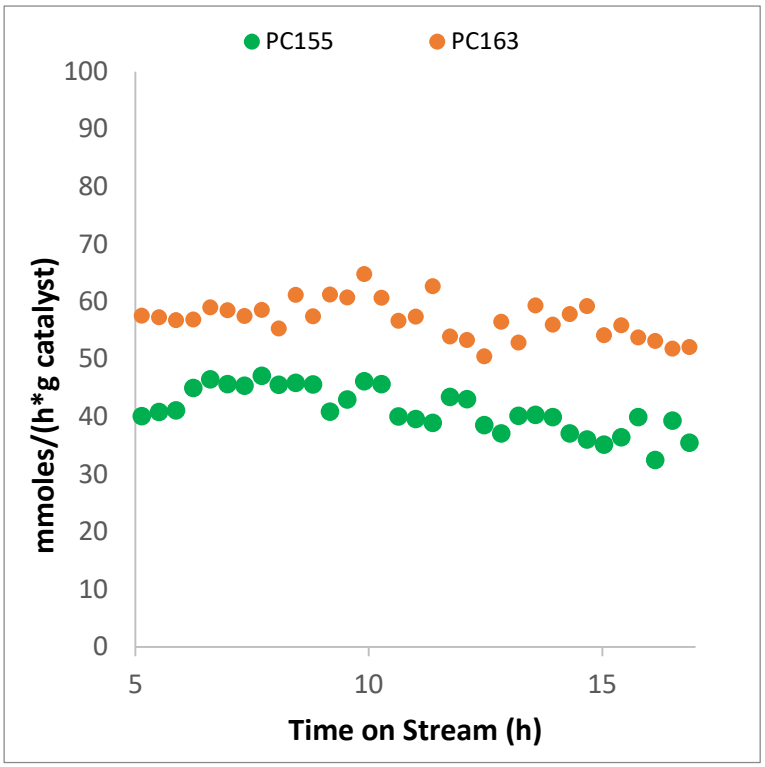

Figure 22 Conversion rates of PC163 compared with PC155 that contains the same amount of Pd metal for comparison

We can observe how these two catalysts show a similar deactivation rate but PC163 has higher conversion rate compared to PC155. This time there is a significant difference in conversion rate which can be attributed to the impregnation method as we observed for the 1%Pd catalysts. Copper content is close to that of PC161 and we can see the effect of this copper in the quantity of products showing high retention times (>12 minutes). This suggests that copper is indeed involved in increasing the selectivity towards longer chain products and that impregnating the catalyst in water rather than in n-hexane enhances the catalytic performance.

6. Discussion

At the beginning of this work, we thought that the Pd was enhancing the acidic properties of the MOF as proposed by Dahao et al. [19] and thus making it more active towards aldolic condensation but the TPD-NH_3 showed in figure 8 seems to suggest otherwise, as a higher Pd loading shows less strong acid sites. This could have different meanings, maybe the key to enhance the MOF activity is having weaker Lewis' acids sites, or maybe it all depends on the hydrogen activation properties of the palladium, allowing the formation of acetaldehyde.

We thought that the palladium ions were grafted on the MOF molecule on a missing linker site, displacing acidic hydrogens, this theory seems supported by the DRIFTS analysis in figure 6 which shows a decrease of intensity in 2 peaks at the right of the graph by increasing the palladium loading.

We were able to observe how various catalysts showed higher activities and slower deactivation rates directly proportional with their thermal stability, with the only exception of PC163 which showed a lower thermal stability but also a higher activity compared to PC155. Since PC163 was impregnated with a different method and also contained a small amount of copper, these differences make the comparison with monometallic catalysts not straightforward. The results on palladium impregnated catalysts confirm that Uio-66 has great potential in ethanol upgrading as it shows that activity towards ethanol and stability towards deactivation are clearly related to the stability of its structure. This result could relate to the number of defects that are present. A lower thermal stability is related to a higher number of defects, perhaps by changing the amount of modulating agent during the synthesis of the Uio-66 we can improve the activity and selectivity towards our target product. Catalysts that showed higher activity also showed higher selectivity towards n-butanol, and catalysts that showed a low selectivity towards acetaldehyde also showed a slower deactivation rate during the reaction. This highlights the relation between structure, acetaldehyde selectivity and deactivation, showing that acetaldehyde might be a key molecule in the deactivation mechanism of the catalyst. Scalbert et Al [30] observed deactivation due to coke formation on top of their catalyst. They related the formation of coke to acetaldehyde condensation into long chain molecules that were susceptible to thermal decomposition. We personally

could observe a carbonaceous residue clogging the line carrying the output stream from the reactor to the GC despite having glass wool at the bottom of the reactor to avoid any small particles to leave the reactor. A gas filter was also present right before the GC highlighting the fact that the particle was formed right inside the GC valve at lower temperatures and pressures (200°C, ambient pressure) than the ones at which the reaction was carried out. This event supports the theory of coke formation which appeared to have happened even outside of the reactor without the catalyst present.

Another possible cause for deactivation/structure disruption might be due to water, the tests carried out on PC155 with SiC and silica gel showed a clear difference in both deactivation rates and activities. Silica gel is known for its hygroscopic properties, its presence in the reactor along with the MOF might delay structure loss by adsorbing the water produced in the reaction of aldolic condensation. This is also supported by the increased selectivity towards dehydration products, as by adsorbing water the equilibrium of the reaction is shifted. The fact that the conversion rate is also affected might suggest a further synergic effect between the MOF and the silica.

Although we were able to observe coalescence of the Pd metal on the MOF, reducing the dispersion, the specific area and thus the enhancing effect on the catalyst by the metal. This effect didn’t seem to be very important towards deactivation as we observed through TEM that most of the smaller particles of Pd coalesced after just 15 hours of reaction, while PC155 having the same Pd content of 4% as the sample used in TEM showed high conversion rates even after 45 hours of reaction.

Another important matter to investigate is the number of long chain products that we observe in catalysts that were also loaded with copper. This result suggest that we can tune the selectivity towards different products by impregnating with different metals. Specifically, copper appeared to enhance the selectivity towards longer chain molecules.

While we observed that different metals impregnated on the MOF brought different products we cannot say the same about the different palladium loadings. Though we

could see how between the various percentages of palladium loading the best appeared to be the 4%, for activity, selectivity and stability.

7. Conclusion

Our findings regarding the effect that palladium has on the catalysts were inconclusive as the coalescence of palladium particles didn't appear to play a crucial role in catalyst deactivation. This subject is in need of further research in order to understand how palladium is involved in activating Uio-66 in ethanol upgrading.

Deactivation of the catalysts can happen in many different ways. We were able to observe that the deactivation rates depended on thermal stability, inert used to dilute the catalyst and acetaldehyde selectivity. We can then say that, structure and defects are a key parameter to produce a better catalyst, as they are responsible for thermal stability. Some of the byproducts of the reaction are also clearly responsible for the deactivation of the catalyst as by using a water adsorbing substance such as silica gel to dilute the catalysts we reduced the deactivation rate. Silica must have a further synergic effect on the catalyst as using it to dilute the MOF affected also selectivity and conversion rate. More studies are needed on this regard in order to better understand how this synergy works and if there are better inert materials to dilute the catalyst and further enhance its catalytic performances.

We saw how a small amount of copper impregnated in the MOF showed an increased selectivity towards longer chain products, this effect can be exploited to produce other important molecules longer than six carbon atoms staring from ethanol, reducing the need to produce them from fossil sources.

These tests showed that this combination of MOF and palladium has a lot of potential in the upgrading of alcohols to produce n-butanol. We discovered that there is an optimal amount of palladium to impregnate the MOF and that its closer to 4% rather than 1 or 7%. As the catalysts impregnated with 4% palladium showed better results than those containing 7%. This confirms that the catalytic activity is not only related to palladium metal but by an interaction between the metal and the MOF. Unfortunately, we weren't able to observe a trend in the thermal stability of the catalysts, the fluctuations in their decomposition temperature appeared to be random. They must be related to something that happened during the impregnation

process as many of the catalysts were prepared starting from the same batch of MOF and showed differences only after impregnation. This could be due to random contaminations in the lab. It’s fundamental to further study this phenomenon as it appeared to be the one that most affected the catalytic performance.

The impregnation method also appeared to have effects on stability, conversion rate and selectivity. This indicates that we are less likely to induce defects or other sources of instability in the structure of the MOF by changing the impregnation method.

References

[1] “European Environment Agency,” 2025. [Online]. Available: https://www.eea.europa.eu/en/analysis/indicators/greenhouse-gas-emissions-from-transport. [Accessed January 2026].

[2] “Eurostat,” [Online]. Available: https://ec.europa.eu/eurostat/web/products-eurostat-news/w/ddn-20251114-1. [Accessed January 2026].

[3] “European Commission,” [Online]. Available: https://climate.ec.europa.eu/eu-action/climate-strategies-targets/2050-long-term-strategy_en. [Accessed January 2026].

[4] “Total Energies,” [Online]. Available: https://totalenergies.com/news/press-releases/totalenergies-energy-outlook-2025. [Accessed January 2026].

[5] “European Environment Agency,” [Online]. Available: https://www.eea.europa.eu/en/analysis/publications/trends-and-projections-in-europe-2025. [Accessed January 2026].

[6] “Table.Briefings,” [Online]. Available: https://table.media/en/climate/news-en/eu-transport-emissions-why-they-could-peak-in-2025. [Accessed January 2026].

[7] “World Resource Institute,” [Online]. Available: https://www.wri.org/insights/4-charts-explain-greenhouse-gas-emissions-countries-and-sectors. [Accessed November 2025].

[8] K. V. S. A. M. D. B. M. R. A. K. K. Z. Ningaraju Gejjiganahalli Ningappa, “Sustainable propulsion and advanced energy-storage systems for net-zero aviation,” *Energy & Environmental Science,* no. 22, 2025.

[9] V. R. v. D. J. M. C. M. S. S. J. F. A. R. Möller, “Annex II: Glossary,” in *Climate Change 2022: Impacts, Adaptation and Vulnerability*, D. R. M. T. E. P. K. M. A. A. M. C. S. L. S. L. V. M. A. O. B. R. H.-O. Pörtner, Ed., Cambridge, Cambridge University Press, 2022, pp. 2897-2930.

[10] R. a. B. S. a. M. L. a. S. R. a. M. D. a. S. O. Howarth, “Introduction: Biofuels and the Environment in the 21st Century,” in *Biofuels: Environmental Consequences and Interactions with Changing Land Use*, Cornell University Library's Initiatives in Publishing (CIP), 2009, pp. 15-36.

[11] E. Barbosa, “Alutal,” [Online]. Available: https://blog.alutal.com.br/en/technical-guides/combustiveis-sustentaveis-aviacao-saf-tendencias-qualidade/. [Accessed January 2026].

[12] “LeadVentGRP,” [Online]. Available: https://www.leadventgrp.com/blog/sustainable-aviation-fuel-production-technologies-and-processes?. [Accessed January 2026].

[13] Z. J. T. M. Z. Bofan Wang, “Sustainable aviation fuels: Key opportunities and challenges in lowering carbon emissions for aviation industry,” *Carbon Capture Science & Technology,* vol. 13, 2024.

[14] F. W. Md Nasir Uddin, “Sustainable Aviation Fuels: A Review of Current Techno Economic Viability and Life Cycle Impacts,” *Energies,* vol. 18, no. 20.

[15] J. S. Susan van Dyk, “International Energy Agency,” January 2024. [Online]. Available: https://www.ieabioenergy.com/wp-content/uploads/2024/06/IEA-Bioenergy-Task-39-SAF-report.pdf. [Accessed January 2026].

[16] “GEVO,” [Online]. Available: https://gevo.com/wp-content/uploads/2023/03/Gevo-WP_aviation-fuel-10.18.22.pdf. [Accessed January 2026].

[17] N. P. Y. H. K. Jane O’Malley, “International Council of Clean Transport,” November 2023. [Online]. Available: https://theicct.org/wp-content/uploads/2023/11/ID-37-%E2%80%93-SAF-Grand-Challenge-white-paper-letter-40036-v3.pdf. [Accessed January 2026].

[18] F. V.-B. L. A. T. R. R. M. C. M. A. Portillo Crespo, “Insights on Guerbet Reaction: Production of Biobutanol From Bioethanol Over a Mg–Al Spinel Catalyst,” *Frontiers in Chemistry,* vol. 10, 2022.

[19] G. F. Y. T. X. W. Y. W. D. H. W. L. Z. L. P. T. L. L. K. X. J. N. X. L. Dahao Jiang, “Multifunctional Pd@UiO-66 Catalysts for Continuous Catalytic Upgrading of Ethanol to n-Butanol,” *ACS Catalysis,* vol. 8, no. 12, 2018.

[20] J. G. S.-H. E. S.-R. G. C. Z. I. F. H. A. J. J. Q.-R. Angel Eduardo García-Hernández, “Sustainable aviation fuel from Butanol: A Study in optimizing Economic and Environmental impact through process intensification,” *Chemical Engineering and Processing - Process Intensification,* vol. 200, 2024.

[21] M. S. C. W. M. W. D. D. Q. H. S. A. M. B. S. S. E. D. S. A. K. Xuetong Pei, “Enhanced stability and activity in the upgrading ethanol to n-butanol using a ruthenium polyphenylene catalyst,” *Applied Catalysis A: General,* vol. 694, 2025.

[22] T. T. A. G. F. C. C. C. D. C. F. P. A. C. F. V. D. D. B. R. M. Andrea Piazzi, “Molecular catalysed Guerbet reaction: Moving to the larger and the Greener through LCA and scale up simulation approaches,” *Sustainable Chemistry and Pharmacy,* vol. 35, 2023.

[23] A. G. C. C. F. C. T. T. F. C. R. M. Alessandro Messori, “Advances in the homogeneous catalyzed alcohols homologation: The mild side of the Guerbet reaction. A mini-review,” *Catalysis Today,* vol. 423, 2023.

[24] X. L. J. D. Y. L. J. L. L. G. X. Z. H. H. Z. L. Huan Tang, “Improving proton conductivity of metal organic framework materials by reducing crystallinity,” *Applied Organic Chemistry,* vol. 36, no. 8, 2022.

[25] R. F. d. L. I. O. ,. P. L. A. M. A. O. I. A.-T. Pedro Cantarero Gómez, “Mechanistic assessments of acetaldehyde aldol condensation under capillary condensation within defective Zr-MOFs,” *Applied Catalysis B: Environment and Energy,* vol. 371, 2025.

[26] P. E. P. C. E. H. R. T. B. W. D. J. Sumit Chakraborty, “Highly Selective Formation of n-Butanol from Ethanol through the Guerbet Process: A Tandem Catalytic Approach,” *Journal of American Chemical Society,* vol. 137, no. 45, 2015.

[27] W. Y. H. B. S. P. V. D. V. A. V. Dries Gabriëls, “Review of catalytic systems and thermodynamics for the Guerbet condensation reaction and challenges for biomass valorization,” *Catalysis Science and Technology,* vol. 5, 2015.

[28] R. J. D. Joseph T. Kozlowski, “Heterogeneous Catalysts for the Guerbet Coupling of Alcohols,” *ACS Catalysis,* vol. 3, no. 7, 2013.

[29] J. M. M. H. J. M. J. K. Karel Frolich, “The utilization of bio-ethanol for production of 1-butanol catalysed by Mg–Al mixed metal oxides enhanced by Cu or Co,” *Clean Technologies and Environmental Policy,* vol. 26, 2023.

[30] F. T.-S. R. J. D. M. F. M. Julien Scalbert, “Ethanol condensation to butanol at high temperatures over a basic heterogeneous catalyst: How relevant is acetaldehyde self-aldolization?,” *Journal of Catalysis,* vol. 311, pp. 28-32, 2014.

[31] G. P. V. J. L. F. D. S. Albert F. B. Bittencourt, “Elucidating the Catalytic Valorization of Ethanol over Hydroxyapatite for Sustainable Butanol Production: A First-Principles Mechanistic Study,” *The Journal of Physical Chemistry C,* vol. 128, no. 35, 2024.

[32] S. J. R. M. Y. A. J. R. M. D. Constanze N. Neumann, “Metal−Organic Framework-Derived Guerbet Catalyst Effectively Differentiates between Ethanol and Butanol,” *Journal of the American Chemical Society,* vol. 141, 2019.

[33] S. S. A. T. B. Christopher R. Ho, “Mechanism and Kinetics of Ethanol Coupling to Butanol over Hydroxyapatite,” *ACS Catalysis,* vol. 6, no. 2, 2015.

[34] V. A. N. A. B. B. R. V. J. L. F. N. T. Makoye Amosi, “Experimental and Kinetic Modelling Study of the Heterogeneous Catalytic Conversion of Bioethanol into n-Butanol Using MgO–Al2O3 Mixed Oxide Catalyst,” *Catalysts,* vol. 15, no. 8, 2025.

[35] S. M. C. Sergio J. Garibay, “Isoreticular synthesis and modification of frameworks with the UiO-66 topology,” *Chemical Communication,* no. 41, 2010.